

Cite this: *Chem. Sci.*, 2023, 14, 13661

Advances in CO₂ activation by frustrated Lewis pairs: from stoichiometric to catalytic reactions

Md. Nasim Khan,^{ab} Yara van Ingen,^a Tribani Boruah,^a Adam McLauchlan,^a Thomas Wirth^{bd} and Rebecca L. Melen^{ba}

The rise of CO₂ concentrations in the environment due to anthropogenic activities results in global warming and threatens the future of humanity and biodiversity. To address excessive CO₂ emissions and its effects on climate change, efforts towards CO₂ capture and conversion into value adduct products such as methane, methanol, acetic acid, and carbonates have grown. Frustrated Lewis pairs (FLPs) can activate small molecules, including CO₂ and convert it into value added products. This review covers recent progress and mechanistic insights into intra- and inter-molecular FLPs comprised of varying Lewis acids and bases (from groups 13, 14, 15 of the periodic table as well as transition metals) that activate CO₂ in stoichiometric and catalytic fashion towards reduced products.

Received 28th July 2023

Accepted 7th November 2023

DOI: 10.1039/d3sc03907b

rsc.li/chemical-science

Introduction

Background

Since the beginning of the industrial revolution, human activity has raised the concentration of carbon dioxide (CO₂), amongst other important greenhouse gases, in the environment by over 50%. CO₂ gas absorbs and emits radiant energy at infrared wavelengths that causes an increase in atmospheric temperature, thus global warming and has become a main driver of climate change.¹ Society has made some progress in finding low-carbon emitting alternatives, for example in sources of energy, and now a scattered dip in CO₂ level has been observed. Minimising CO₂ emissions by at least 50% to limit the increase in the global average temperature by 2 °C by 2050 has been set as a global target.² This will require a rapid exploitation of new energy technologies with a low-carbon or zero-carbon energy sources to restore our ecosystem. As one single technology is not expected to solve this problem, global warming alerts have drawn urgent attention to control the expansion of CO₂ concentrations in the atmosphere through the framework of carbon capture, storage, and utilisation (CCSU).³ The important challenge remains not only in carbon dioxide capture and storage but also to utilise it for the creation of value-added carbon products.⁴ CCSU processes add value to the conversion of CO₂ into fuels and chemicals, and can compensate the cost of capturing CO₂. This approach has generated many new directions in various branches of science and technologies including chemical, biological and material applications.⁵ Extensive work

has been carried out in the past few decades for CO₂ capture and utilisation (CO₂-CU) using various chemical processes for the reduction of CO₂ into products such as formic acid and methanol, or light hydrocarbons such as methane.⁶ Metal and non-metal derived reagents and catalysts in homogeneous and heterogeneous systems have been explored including promising mediums such as zeolites, metal-organic frameworks (MOFs), covalent organic frameworks (COFs), nanomaterials, as well as electrochemical, photochemical and thermal processes.

The activation and chemical conversion of CO₂ requires high energy due to its high thermodynamic stability ($\Delta G_f^\circ = -396 \text{ kJ mol}^{-1}$).⁷ Entropy is one important factor that limits CO₂ transformations, even for some reactions where $\Delta H^\circ < 0$, ΔG° is positive. Conversion of CO₂ can take place at room temperature or at lower temperatures but in such transformations the carbon atom retains its oxidation state of +4 and promotes the formation of carbamates, carbonates, urea and its derivatives, polycarbonates, and polyethers, where OH⁻, H₂O, amines, carbanions, olefins, alkynes, and dienes have been reacted as reagents with CO₂. Reactions that produce carboxylates from CO₂ are thermodynamically favourable. Carbon product formation such as methanol, carbon monoxide, formaldehyde, methane, and hydrocarbons from CO₂ require higher energy, and thus kinetic control to steer away from the thermodynamically favoured products. Kinetically, to obtain CO₂ reduced products with a change of oxidation state in the carbon atom requires more energy. To achieve the reduction of CO₂, the reagent should bend CO₂ to overcome the first energy barrier and to achieve subsequent reduction steps. Preorganised reducing agents kinetically favour the challenging reduction of CO₂ beyond carbonate or formate.

To overcome the energy barrier, external sources of energy (such as electrochemical, photochemical or thermal energy) are

^aCardiff Catalysis Institute, School of Chemistry, Cardiff University, Translational Research Hub, Maindy Road, Cathays, Cardiff, CF24 4HQ Cymru/Wales, UK. E-mail: MelenR@cardiff.ac.uk

^bSchool of Chemistry, Cardiff University, Main Building, Park Place, Cardiff CF10 3AT, Cymru/Wales, UK. E-mail: wirthT@cardiff.ac.uk



typically required. If value-added products are obtained at higher cost compared to the cost of CO₂ capturing and natural fuels, then the process would not be economical and could not be applied industrially.⁸

Although CO₂ has been reduced to obtain chemicals and fuels, the current use of CO₂ in chemical synthesis is limited owing to the high thermodynamic stability of CO₂ that has to be overcome.⁹ To control the energy barrier in reduction processes of CO₂, metals are being used that are often rare and high cost materials, indeed transition metals are being explored making the process efficient and cost effective. The conversion of CO₂ to value-added products is highly desirable, yet the inert and highly energetically stable nature of this small molecule makes this a challenging task.¹⁰ CO₂ is a linear and an apolar molecule (dipole moment, $\mu = 0$), despite its two polar C=O bonds and is ambiphilic in nature. The length of the C=O bond in CO₂ is 116.3 pm, shorter than the approximate 140 pm bond length of a typical single C–O bond, and shorter than most other C=O double bonds, such as carbonyls.¹¹ It offers two reaction sites, an electrophilic site at the carbon (Lewis acidic centre) due to the low-lying empty antibonding π^* orbital (LUMO, lowest unoccupied molecular orbital), and two nucleophilic sites at the oxygen atoms (Lewis basic character) due to an available pair of valence electrons (HOMO, highest occupied molecular orbital) (Fig. 1). Carbon dioxide has an electron affinity (E_{ea}) of about -0.6 eV and a first ionisation potential (IP) of about $+13.8$ eV which makes it a better electron acceptor than electron donor. Overall, a high energy of about 750 kJ mol⁻¹ is required to break the C=O bond. Upon activation, the molecule will distort from its linear sp-hybridised geometry to a sp²-hybridised carbon centre with concurrent elongation of the C=O bond and a change in its molecular energy.¹²

Classical activation of CO₂ by nucleophilic attack at the carbon atom can be achieved using bases,¹³ transition metals,¹⁴ or by one electron reductions¹⁵ to ultimately generate acetates, carbamates, ureas, bicarbonates, oxalates, formates, or carbon monoxide, amongst other products (Fig. 2). Further advances in research have been able to achieve value added carbon products by reducing CO₂ to products such as methanol, methane, or higher carbon chains.¹⁶

Frustrated Lewis pairs (FLPs)¹⁷ are mixtures of a Lewis acid and a Lewis base, that, because of steric hindrance, cannot combine to form a classical adduct. FLPs can perform efficient chemical transformations without losing the individual properties of the FLP system.¹⁸ This feature also enables the activation of small molecules including CO₂ and is now well-explored



Fig. 1 Molecular properties of carbon dioxide.



Fig. 2 Classical activation reactions of carbon dioxide.

in the literature in several reviews.¹⁹ Herein, we cover all major developments made using p-block elements and transition metals to activate CO₂ with FLP systems with a particular emphasis on more recent reports. In this review we will cover stoichiometric as well as catalytic processes including theoretical efforts to understand the mechanism of CO₂ activation and reduction using FLPs.

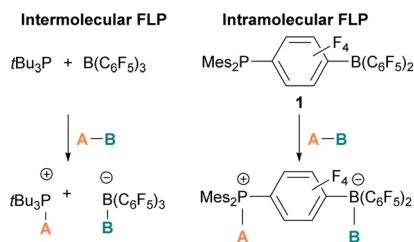
Frustrated Lewis pairs (FLPs)

In the classic model of Gilbert Lewis (Fig. 3a), a Lewis base with an electron pair in the HOMO donates electron density to the LUMO of the Lewis acid by forming a dative bond.²⁰ This process provides a HOMO of lower energy with a stabilised donor acceptor adduct and quenches the reactivity of both, the Lewis acid and base. A deviation to the classical model was observed after the augmented work reported by Brown,²¹ in which no adduct formation occurred between BMe₃ and 2,6-lutidine, and later Wittig,²² Tochtermann,²³ Piers²⁴ and Oestreich.²⁵ Stephan and co-workers coined the chemical term “frustrated Lewis pair” (FLP) that exists with unquenched acidity and basicity in a combination of a sterically hindered Lewis acid and Lewis base (Fig. 3b).²⁶ This inhibition of adduct formation allows for the HOMO of the Lewis base and the LUMO of the Lewis acid to effect non-classical reactivity.

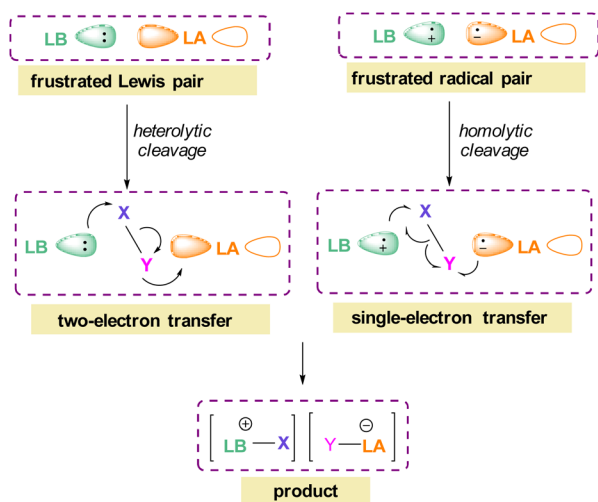


Fig. 3 Frontier molecular orbital presentation of (a) a classic Lewis acid–base adduct and (b) a frustrated Lewis pair. LA = Lewis acid; LB = Lewis base.





Scheme 1 Cleavage of molecule A–B with intermolecular and intramolecular FLPs. Mes = Mesityl.



Scheme 2 FLP reactivity with small molecules via heterolytic (two e^- transfer) and homolytic cleavage (single e^- transfer).

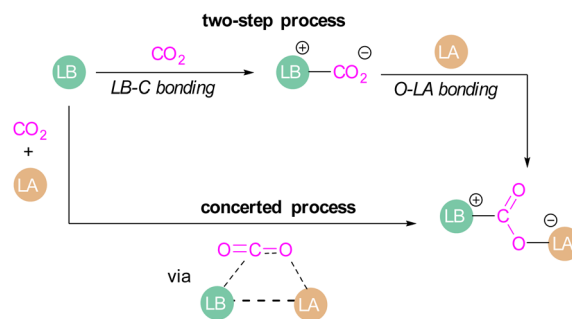
The pioneering work of splitting dihydrogen heterolytically with the FLP $t\text{Bu}_3\text{P}/\text{B}(\text{C}_6\text{F}_5)_3$ demonstrated that the unquenched reactivity of FLPs could be applied to the activation of small molecules.²⁷ Since then, various FLP systems have been investigated to activate a variety of small molecules. Two types of FLP systems are typically considered: intermolecular or intramolecular (Scheme 1). Intermolecular FLPs are systems where the Lewis acid and Lewis base are two individual molecules that interact through secondary London dispersion interactions to bring the Lewis acid and base together where small molecules insert into the cavity of the FLP such as the combination of $t\text{Bu}_3\text{P}$ and $\text{B}(\text{C}_6\text{F}_5)_3$. In intramolecular FLP systems, the Lewis acid and Lewis base are combined in one molecule by a covalent linker. An example of an intramolecular FLP system is the phoshinoborane **1** shown in Scheme 1, where the Lewis acidic boron centre and the Lewis basic phosphorus centre are separated by an aryl ring. These molecules are also able to heterolytically cleave the bonds in small molecules, the Lewis base donates its electron pair to the electron deficient fragment of the small molecule and the Lewis acid accepts an electron pair from the HOMO of the small molecule. This results in bond formation and an ionic/zwitterionic product. It has also been found that certain combinations of Lewis acids

and bases in FLPs can lead to a transfer of one electron from the Lewis basic donor to a Lewis acidic acceptor generating a reactive frustrated radical pair (FRP). This FRP can react in a homolytic way with small molecules (Scheme 2).²⁸

Mechanistic aspects of FLP CO_2 reduction

Amongst the small molecules activated by FLPs, CO_2 has been well-studied owing to the importance of discovering new CCSU processes. Two mechanistic pathways are proposed for the capture and activation of CO_2 by FLPs thus far (Scheme 3). One is a concerted mechanism and the other is a two-step process. Two computational models have been explored in the $t\text{Bu}_3\text{P}/\text{B}(\text{C}_6\text{F}_5)_3$ FLP system to study the mode of CO_2 activation. In the concerted mechanism, the reactants (FLP and free CO_2) and the CO_2 -FLP adduct is formed by a single transition state (TS) in which the LB–C and LA–O bonds are formed simultaneously.²⁹ Conversely, for the two-step process, when the CO_2 moves closer to the FLP system, the P–C bond is formed first, followed by the formation of the B–O bond to give the final CO_2 -FLP adduct.

It is well-documented that the solvent is important to stabilise the final zwitterionic products.³⁰ Liu and co-worker³¹ led a mechanistic study in the solid-state utilising density functional theory (DFT) simulations, in which they analysed the separate roles of the Lewis acid and base without the presence of a solvent. The authors found that the reaction proceeds in a two-step process where CO_2 initially enters the cavity of the $t\text{Bu}_3\text{P}/\text{B}(\text{C}_6\text{F}_5)_3$ FLP. The carbon atom of CO_2 then interacts with the phosphorus atom and an oxygen atom interacts with boron leading to a reduction in the O–C–O angle of CO_2 to 167.8° . This means that the CO_2 species is bent although there are no chemical bonds formed. They believe that this is due to a weak interaction between CO_2 and the FLP, where CO_2 interacts with crystal fields in the solid state created by the FLP pair. In the solution state, the crystal fields would be replaced by solvent interactions. In studying the separate roles of the Lewis acid and base, the authors suggest that the combination of a strong Lewis acid and a weak Lewis base should be selected to make the CO_2 activation thermodynamically feasible. This is due to the formation of the B–O bond being strongly exergonic while the formation of the P–C bond was deduced to be endergonic.



Scheme 3 Mechanistic aspects of FLPs in their reaction with CO_2 .





Scheme 4 Electrochemical reduction of FLP adduct $t\text{Bu}_3\text{P-CO}_2\text{-B}(\text{C}_6\text{F}_5)_3$.

Other sources of energy such as light and/or electric current have been employed in other fields however, the most used source of energy for the activation of CO_2 with FLP systems is heat and pressure of CO_2 .

However, in the FLP adduct of CO_2 , the CO_2 molecule is bent, and a one-electron transfer could facilitate the reduction process. In a homogeneous system, the first electrochemical study was performed on the FLP- CO_2 adduct for $t\text{Bu}_3\text{P-CO}_2\text{-B}(\text{C}_6\text{F}_5)_3$ (Scheme 4).³² Electrochemically, when an electron is added to $t\text{Bu}_3\text{P-CO}_2\text{-B}(\text{C}_6\text{F}_5)_3$, a change in the bond lengths was observed. The carbon oxygen $\text{C}=\text{O}$ bond length increased by 0.05 Å in and the $\text{C}-\text{O}$ bond length decreased by 0.03 Å. The $\text{B}-\text{O}$ and $\text{P}-\text{C}$ bonds both decreased in length by 0.06 Å and 0.01 Å, respectively. Overall, it was observed that addition of electrons to the CO_2 adduct $t\text{Bu}_3\text{P-CO}_2\text{-B}(\text{C}_6\text{F}_5)_3$ first generated intermediate $[t\text{Bu}_3\text{P-CO}_2\text{-B}(\text{C}_6\text{F}_5)_3]^-$, then reduced CO_2 to CO also generating $t\text{Bu}_3\text{P}$, and $[(\text{HO})\text{B}(\text{C}_6\text{F}_5)_3]^-$. In this system, the intermediate $[t\text{Bu}_3\text{P-CO}_2\text{-B}(\text{C}_6\text{F}_5)_3]^-$ can also react with the solvent THF causing dimerisation.

To obtain a controlled reduction of CO_2 , FLPs in the solid-state have been explored based on the phenomenon of adsorption, activation, and evolution pathways of CO_2 . For example, Yan and co-workers created a stable FLP system for the activation of carbon dioxide.³³ Their system involves a composite material of zinc and tin having different electronegativities. The Lewis pairs first capture and stabilise protons and then selectively activate CO_2 . Here the zinc oxide surface captures protons and acts as a Lewis base while the tin acts as Lewis acid. The two-electron reduction with two protons start the reaction for CO_2 activation and finally resulted in the formation of formic acid.

In this review we will cover FLP mediated activation and reduction of CO_2 that has been explored to achieve value-added carbon products. This will include, several inter- and intramolecular FLPs systems which have been designed and developed utilising both p- and d-block elements acting as a Lewis acid in combinations with p- and d-block elements acting as a Lewis base. Each section and sub-sections will detail the different systems developed with stoichiometric and catalytic quantities of FLPs, and will be ordered by the periodic group of the Lewis acid to give structure to this review. The mechanistic and computational insights will be discussed where relevant.

Group 13 Lewis acids

Borane/phosphine FLPs for CO_2 activation

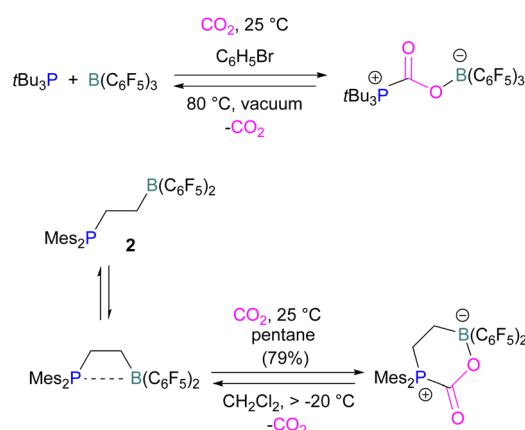
Boron is by far the most explored Lewis acidic element in FLPs for CO_2 activation. Different Lewis base partners such as

phosphorous, nitrogen, carbon as a carbene and metals have been explored in combination with the boron Lewis acid.

Many of the first FLP systems for CO_2 activation involved phosphorus as the Lewis basic component. Early FLPs utilised in CO_2 activation comprised of a phosphine and borane that could reversibly bind and release CO_2 including the intermolecular FLP $t\text{Bu}_3\text{P/B}(\text{C}_6\text{F}_5)_3$ and **2** (Scheme 5).

At the time, these systems offered rare examples of metal-free CO_2 sequestration.³⁴ Theoretical investigations show the mechanism proceeding by simultaneous formation of $\text{P}-\text{C}$ and $\text{O}-\text{B}$ bonds from thermochemical computed data (B97-D/TZVPP', B2PLYP-D/TZVPP', and B2PLYP-D/QZVP(-g, -f) levels of theory). $t\text{Bu}_3\text{P}$ reacts with $\text{B}(\text{C}_6\text{F}_5)_3$ at room temperature and under 1 bar of CO_2 forms the desired stable product $t\text{Bu}_3\text{P-CO}_2\text{-B}(\text{C}_6\text{F}_5)_3$, which upon heating at 80 °C under vacuum releases the CO_2 molecule and regenerates the starting FLP mixture. Calculations for the formation of $t\text{Bu}_3\text{P-CO}_2\text{-B}(\text{C}_6\text{F}_5)_3$ show that the overall reaction is exothermic. Privalov and co-workers calculated several energy pathways for CO_2 activation.³⁵ After these first reports of non-metal based inter- and intramolecular FLP-mediated reversible CO_2 activation, the scientific community explored a range of new FLPs for CO_2 activation, as shown in Fig. 4. Several other phosphine bases and boron acids have been used in the intermolecular system including $i\text{Pr}_3\text{P}$, XPhos and Mes_2EtP , and $\text{B}(p\text{-C}_6\text{F}_4\text{H})_3$, and $\text{B}(\text{R})(\text{C}_6\text{F}_4\text{H})_2$, (R = hexyl, Cl, cyclohexyl, norbornyl, Ph).^{36,37} More complex boranes bearing functionalised substituents with cyclic structures were also tested with $t\text{Bu}_3\text{P}$ to trap CO_2 generating adducts **3** and **4**.³⁸

Interestingly, when $(\text{Me}_3\text{Si})_3\text{P}$ was utilised as a Lewis base instead of $t\text{Bu}_3\text{P}$, with $\text{B}(p\text{-C}_6\text{F}_4\text{H})_3$, silyl migration was observed in the final adducts **5** and **6** (Fig. 4 and Scheme 6). $t\text{Bu}_3\text{P}$ and $(\text{Me}_3\text{Si})_3\text{P}$ with CO_2 in pentane at room temperature initially yields the expected adduct $(\text{Me}_3\text{Si})_3\text{P-CO}_2\text{-B}(p\text{-C}_6\text{F}_4\text{H})_3$. Subsequently, silyl migration from phosphorus to oxygen forms a stable compound which can be better represented as the zwitterionic compound **5**. The same starting Lewis acid and base can also react with two equivalents of CO_2 in dichloromethane (CH_2Cl_2) at room temperature for 24 h, providing silyl migrated product **6**. Compound **6** can also be obtained from **5**,



Scheme 5 First inter- and intramolecular FLPs utilised in CO_2 activation.



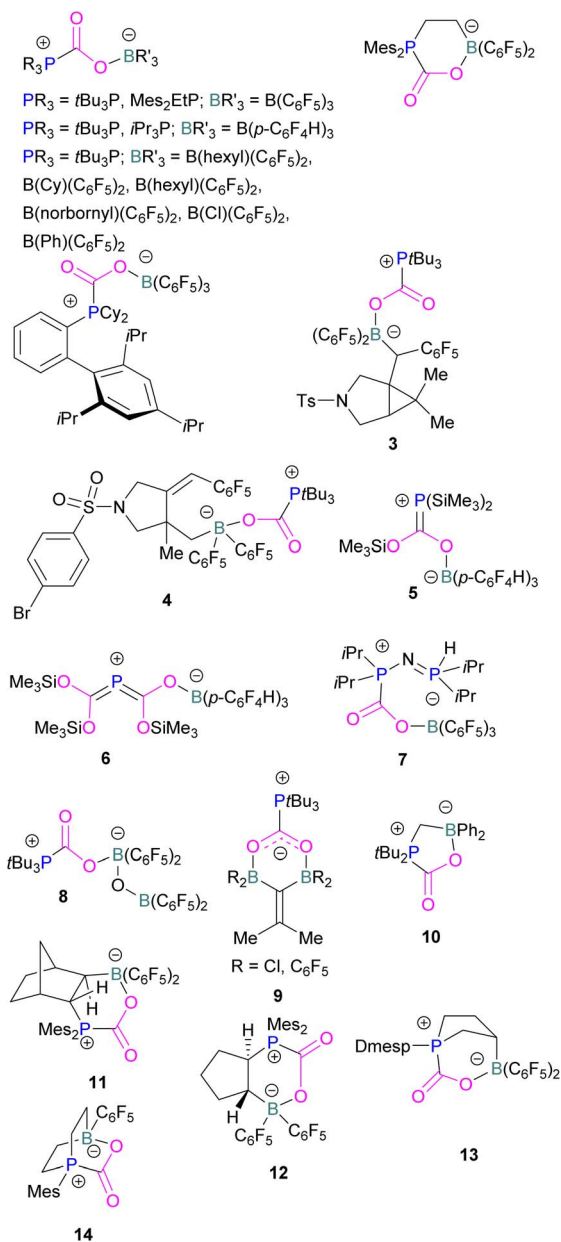
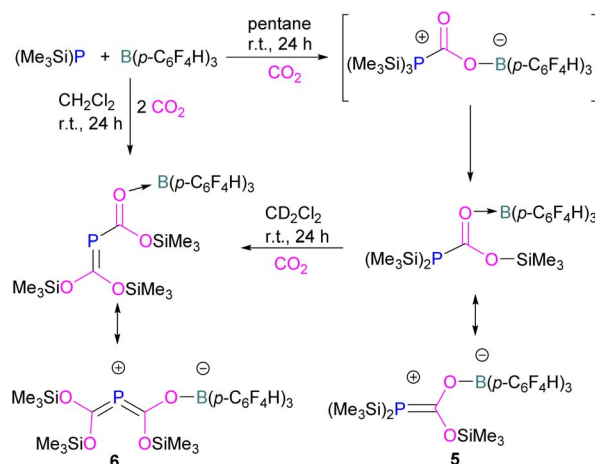


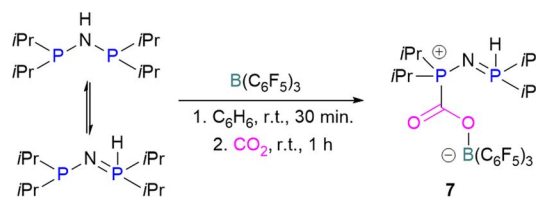
Fig. 4 Examples of FLP adducts of boranes with a phosphorus Lewis base. Dmesp = Dimesitylphenyl.

when **5** is treated with CO_2 in CD_2Cl_2 at room temperature for 24 h (Scheme 6).³⁹ Kemp and co-workers on the other hand, investigated the phosphine base bis(di-*i*-propylphosphino) amine with $B(C_6F_5)_3$ which formed the expected 1 : 1 adduct **7**. The crystal structure of **7** shows that H-isomerisation took place with a migration of the proton from nitrogen to phosphorus (Scheme 7).⁴⁰

Stephan and co-workers have expanded the borane scope to explore the reactivity of bis-boranes to trap CO_2 with tBu_3P . It was also found that, 1,1-bis- $(C_6F_5)_2BOB(C_6F_5)_2$ binds with CO_2 in a monodentate manner generating **8**, whilst bis-boranes of type $(R_2B)_2C=CMe_2$, where $R = Cl$ or C_6F_5 , provide a bidentate chelation of CO_2 to obtain a unique type of heterocyclic



Scheme 6 Silyl migration in the $(Me_3Si)_3P$ and $B(p-C_6F_4H)_3$ FLP.



Scheme 7 H-isomerisation with a migration of the proton from nitrogen to phosphorus.

compounds **9**.⁴¹ The chelation of CO_2 by the two B-centres in **8** was restrained due to steric crowding as well as a significant π -character in the B–O bonds, which was evident from the relatively large B–O–B bond angle of $139.5(2)^\circ$. Whereas, in **9** B–C–B angles of $117.3(2)^\circ$ ($R = Cl$) and $121.2(2)^\circ$ ($R = C_6F_5$) show a six membered planar structure.

In intramolecular systems, when the Lewis base and acid are sufficiently aligned in a geminal fashion, an increase in reactivity is observed as seen in the formation of adduct **10**.⁴² Another intramolecular FLP with a norbornane structure with a vicinal designed FLP was utilised to trap CO_2 to obtain adduct **11**.⁴³ Similarly to the vicinal FLP in adduct **11**, an FLP based on cyclopentane with *trans*-1,2-substituents was explored to form **12**.⁴⁴ Other intramolecular B/P FLP systems include an active FLP borylated tetrahydrophosphole which yielded adduct **13**,⁴⁵ and a cyclic six membered FLP with 1,4-phosphane/borane substituents which undergoes an addition reaction with CO_2 to form adduct **14**. Erker and co-workers observed that heating **14** in *n*-heptane at $80^\circ C$ for 15 min under CO_2 converts **14** to its cyclotetrameric macrocyclic oligomer **15**. Tetramer **15** is unstable in solution, even in a CO_2 atmosphere it slowly converts back to the monomer **14** (Fig. 5).⁴⁶

Szynkiewicz and co-workers reported the phosphinoboration and diphosphination of CO_2 . In 2019, they published the first report of catalytic (with respect to the borane) diphosphination of CO_2 with a diphosphane/boron FLP. CO_2 was inserted into the relatively weak P–P bond (Scheme 8).⁴⁷ Furthermore in 2019, they reported the use of diamino-phosphinoboranes to





Fig. 5 FLP adducts of boranes with P-base. Mes* = 2,4,6-Tri-*tert*-butylphenyl.



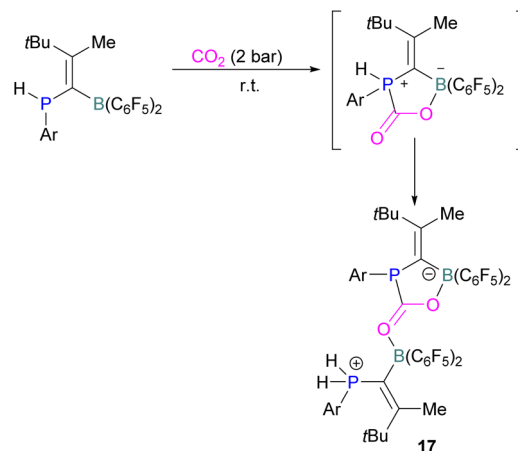
Scheme 8 Diphosphination (top) and phosphinoboration (bottom) of CO₂.

phosphinoborate CO₂; though not sterically frustrated, this compound still exhibits FLP-like reactivity (Scheme 8, bottom).⁴⁸ More recently the same group built on this work, reporting the reaction of CO₂ (among several other small molecules) with a diphosphinoborane B(P*t*Bu₂)₂Ph to yield a diphospha-urea and a bicyclic diboroxane **16** (Scheme 9). The reaction proceeds by CO₂ insertion into a single B–P bond, elimination of (*t*Bu₂P)₂C=O to give phenyl oxoborane PhBO. Reaction of this species with a further equivalent of the parent diphosphinoborane and 2 equivalents of CO₂ gives the product **16**. While stable under N₂, the product decomposes with loss of CO₂ and diphospha-urea to give triphenylboroxine (PhBO)₃.⁴⁹

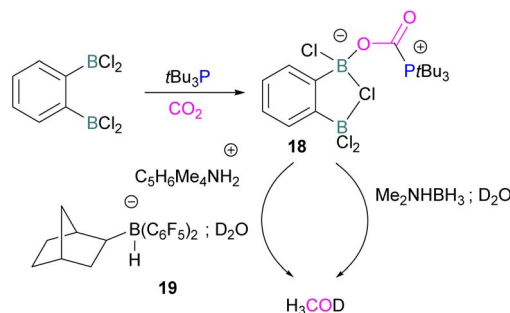
Kesete and co-workers published a computational study evaluating a number of intramolecular phosphine/borane catalysts for CO₂ reduction. One finding was that, though electron-withdrawing substituents on borane like fluorine stabilise the CO₂-FLP adduct, they also destabilise the transition state (TS), increasing activation energy. Fluorination of the substituents of the phosphorus reduces its basicity and so destabilises both the transition state and the adduct formed. This highlights the importance of tuning the Lewis acidic and

basic sites of FLPs to achieve stabilised transition states, but that are also Lewis acidic, or Lewis basic enough centres to bind with CO₂.⁵⁰ Jian and co-workers reported in 2017 that geminal vinylidene-bridged phosphorus/boron Lewis pairs could react with CO₂ to give a phosphinodiborated product **17**, as shown in Scheme 10. Interestingly, this geminal P/B is supported with an sp² carbon, which is different from previous reports of geminal FLPs.⁵¹

Following activation of CO₂, the subsequent transformations have been investigated initially stoichiometrically. Stephan and co-workers reported that the bis-borane, 1,2-C₆H₄(BCl₂)₂, forms an adduct with *t*Bu₃P and also shows FLP reactivity with CO₂ to form the FLP-CO₂ zwitterionic compound **18** (Scheme 11). Compound **18** is remarkably more stable, with respect to the loss of CO₂, and no decomposition was observed even on heating to 80 °C for 24 h compared to the CO₂ adducts obtained from FLPs *t*Bu₃P/B(C₆F₅)₃ (loss of CO₂ at 80 °C), Mes₂PCH₂-CH₂B(C₆F₅)₂ (loss of CO₂ at –20 °C), and bis-boranes Me₂C=C(BR₂)₂ where R=Cl, C₆F₅ with *t*Bu₃P (loss of CO₂ at 15 °C). The chlorine atom in **18** bridges between the boron centres which enhances the Lewis acidity of the boron bound with the oxygen atom of CO₂ and results in a stronger B–O bond making the adduct more thermally stable, than other discussed examples. Hence, the strength of the bond between the Lewis acid and the



Scheme 10 Reaction of geminal vinylidene-bridged P/B Lewis pair with CO₂.



Scheme 11 Stoichiometric reduction of FLP-CO₂ adduct **18**.

Scheme 9 Synthesis of phenyl oxoborane.

oxygen atom of CO₂ plays a critical role in establishing reversibility, this can be induced by the addition of electron-withdrawing groups, such as Cl in **18**. The species **18** was reduced by Me₂NHBH₃ followed by quenching with deuterated water (D₂O) to obtain deuterated methanol (MeOD) as the final product. In another way, **18** was also reduced by [C₅H₆Me₄NH₂]/[HB(C₆F₅)₂(C₇H₁₁)] (**19**) and quenched with D₂O again yielding H₃COD (Scheme 11). Here, two Lewis acidic boron sites are available, and bridging of a chlorine atom between the two stabilises the zwitterionic adduct.⁵²

There remain two major issues with *t*Bu₃P/1,2-C₆H₄(BCl₂)₂ that pose limitations for a catalytic cycle. The first issue is that H₂ cannot be activated, so H₂ surrogates such as Me₂NHBH₃ or [C₅H₆Me₄NH₂]/[HB(C₆F₅)₂(C₇H₁₁)] were utilised as stoichiometric reductants. Secondly, the boron centre in this FLP is more oxophilic, so the last step required quenching with D₂O to cleave the B–O bond.

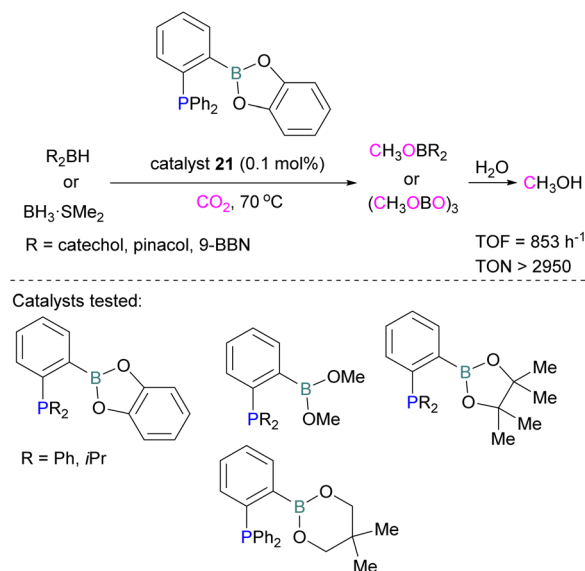
In another stoichiometric system, O'Hare and co-workers synthesised a series of FLPs based on Lewis acid {C₆F₄(*o*-C₆F₅)₃B and (C₆Cl₅)₃B with trialkylphosphines as Lewis bases (Scheme 12). The idea of synthesising these FLPs was to achieve a weaker B–O bond to facilitate the cleavage of B–O bond upon reduction and potentially generate a catalytic system. The steric congestion factor was applied as steric bulk at the *ortho* position alone could decrease the B–O bond strength.⁵³ The synthesised FLPs were exposed to H₂ to form FLP-H₂ as activated salts of the type [R₃P-H][H-BR₃]. These salts were then exposed to CO₂ (1 atm) to obtain formatoborates of type **20** in the presence of toluene at 140 °C for 24 h using Young's tap NMR tubes. The formatoborates **20** could also be prepared independently from the reaction of the FLP with formic acid in toluene at room temperature for 16 h (Scheme 12).⁵⁴ The formatoborates **20** were subjected to H₂ and heated to 140 °C for 16 h but were not reduced, instead decarboxylation of the formatoborates **20** occurred and hydride salts were formed with no further reductions.

The higher stability of the formatoborates **20** and their decarboxylation at higher temperatures limited this FLP approach for a catalytic reduction of CO₂.

Following reports on stoichiometric reactions, the first catalytic reduction of CO₂ with an organocatalyst FLP was explored by Fontaine and co-workers in 2013. They applied hydroboranes HBR₂ [HBcat (catecholborane), HBpin (pinacolborane), 9-BBN (9-borabicyclo[3.3.1]nonane), BH₃·SMe₂ and BH₃·THF] to produce CH₃OBR₂ or (CH₃OBO)₃ following reduction of CO₂. Upon hydrolysis, CH₃OBR₂ or (CH₃OBO)₃



Scheme 12 A series of FLPs consisting of C₆F₄(*o*-C₆F₅)₃B or (C₆Cl₅)₃B with trialkylphosphines, and their reduction reactions.



Scheme 13 Catalytic performance of **21** in reduction of CO₂ for methanol synthesis (top), and different FLP catalysts tested (bottom).

yield methanol as the final product in up to 99% yield (Scheme 13) with high turnover numbers (TON > 2950) and turnover frequencies (TOF = 853 h⁻¹). The intramolecular phosphino-borane catalyst **21** was found to be an efficient catalyst for this reaction.⁵⁵ The same authors studied the mechanism of this hydroboration of CO₂ with catalyst **21** using computational and experimental methods. It was found that an intramolecular FLP was involved in every step of the reduction and the simultaneous activation of both, the reducing agent and CO₂, were the key to efficient catalysis in every reduction step.⁵⁶ Furthermore, Fontaine and co-workers synthesised various phosphine-borane derivatives of catalyst **21** with different substituents on boron and phosphorus as shown in Scheme 13 (bottom). These were then tested for hydroboration of CO₂ using HBcat or BH₃·SMe₂ to generate methoxyboranes. The most active species were derivatives with a catechol unit on boron. They also performed isotope labelling experiments and DFT studies and found that once the formaldehyde adduct was generated, the CH₂O moiety remained on the catalyst system. The lowest energy barriers were found for concerted activation of catecholborane by the Lewis base and of CO₂ by the Lewis acid. The results show higher potency of “O” for the activation of hydroboranes than “P”.⁵⁷ Overall, FLP **21** acted as an efficient catalyst because of two important features: Firstly, **21** did not form an adduct with CO₂, as seen previously with most FLPs that formed a stable CO₂ adduct. Exposing **21** to 1 atm of CO₂ at room temperature resulted in no spectroscopic change of the solution (by ¹H, ³¹P, and ¹¹B NMR spectroscopy). Also, species **21** remained monomeric in solution without any P–B interaction. Secondly, the CH₂O moiety was released upon reduction from the catalyst and made **21** available for another reaction. Hence, the higher high turnover numbers and high turnover frequencies for **21**. Later, Stephan and co-workers developed another catalytic method for the reduction of CO₂ using 9-BBN



Scheme 14 Phosphine catalysed CO₂ reduction with 9-BBN.

as a reducing agent and phosphine as a catalyst (Scheme 14). The reaction proceeds *via* an FLP-type CO₂ activation intermediate 22 and the reduction products include boron-bound formate species, 23, the diolate-linked compound 24, and methoxide product 25. Intermediate 26 could be transferred to 25 in the presence of 9-BBN and to 27 in the presence of the boron-bound formate species 23. Derivatives of 27 were isolated and confirmed with single crystal X-ray diffraction analysis. With 0.02 mol% of *t*Bu₃P, product 25 is obtained in 98% yield at reaction temperature 60 °C. In the best scenario, the catalyst *t*Bu₃P provides 5556 turnovers of hydride transfers to CO₂ and a TOF of 176 h⁻¹.⁵⁸

Instead of forming a classical adduct of *t*Bu₃P and 9-BBN, this system showed an FLP-type CO₂ activation and subsequent hydride transfer from boron to the carbonyl carbon in 22, releasing *t*Bu₃P for the next cycle and hence this system worked catalytically for the reduction of CO₂.

Dang and co-workers reported a theoretical study on a catalytic mechanism for computationally designed bridged P/B FLPs in the activation of H₂ and CO₂. They found that the reaction follows a one-step concerted mechanism with small reaction barriers (14.8–24.0 kcal mol⁻¹). Among the computationally designed bridged FLPs, some were found to successfully reduce CO₂ with molecular hydrogen in two feasible pathways. The first pathway follows immediate hydrogenation of CO₂ after H₂ activation (Scheme 15, top), the second follows CO₂ activation first, then metathesis of H₂ followed by reductive elimination (Scheme 15, bottom). Both catalytic cycles provide the product HCO₂H from the reduction of CO₂. From all computationally designed bridged FLPs, straightforward H₂ activation takes place with those that do not have electron

Scheme 15 Two different calculated reduction cycles for CO₂ in bridged FLPs.

donating substitutions on the B's adjacent carbon site, or have a long chain between the B and P.⁵⁹

Xanthene FLPs were computationally investigated using DFT methods [level of theory: B3LYP-D3/6-311+G*(*)/M06-2X/6-31G*(*) in bromobenzene], and their reduction of CO₂ was modelled as shown in Scheme 16. Differently substituted

Scheme 16 Xanthene FLPs mediated catalytic reduction of CO₂ into formic acid.

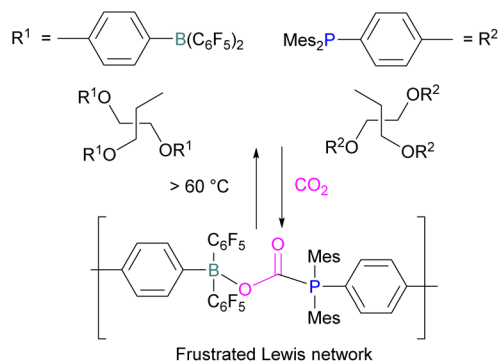
xantheno backbones were investigated, showing that more rigid backbones have lower activation energies for CO₂ hydrogenation.

The formation of P/B-H in the first step was shown to be exergonic and this first intermediate is the catalyst resting stage.⁶⁰ The hydride transfer from boron to the carbonyl carbon of CO₂ produces formate and subsequent protonation resulted in the formation of formic acid bringing the xantheno FLP into the next cycle for the CO₂ reduction.

The incorporation of FLPs into polymers has also seen some success in CO₂ activation. Shaver and co-workers explored the first use of polymeric FLPs to catalyse the incorporation of CO₂ into cyclic ethers for the formation of cyclic carbonates and showed good selectivity (Scheme 17, top). Different phosphines and boranes were explored as the Lewis base and acid in the polymer (Scheme 17, bottom). These poly(FLPs) can easily be recovered and reused after the reaction, however the efficiency of the catalyst gradually decreases due to partial phosphine oxidation and increased crosslinking.⁶¹

Yan and co-workers developed CO₂-responsive dynamic gel system based on an FLP for the first time (Scheme 18). Here, CO₂ can be regarded as a “gas glue” which crosslinks the Lewis acidic and Lewis basic sites and forms a new type of a FLP network. The trapped CO₂ FLP network undergoes reversible release of CO₂ upon heating at >60 °C.

The authors found that CO₂-bridging crosslinks in the network are dynamic covalent linkages, which provides the gel with unique gas-tunable viscoelastic, mechanical, and self-healing characteristics.⁶² The authors showed that the same (-B-CO₂-P-) poly-FLPs are efficient catalysts in transforming amine substrates to formamide derivatives using the CO₂ poly-FLP as the starting point.

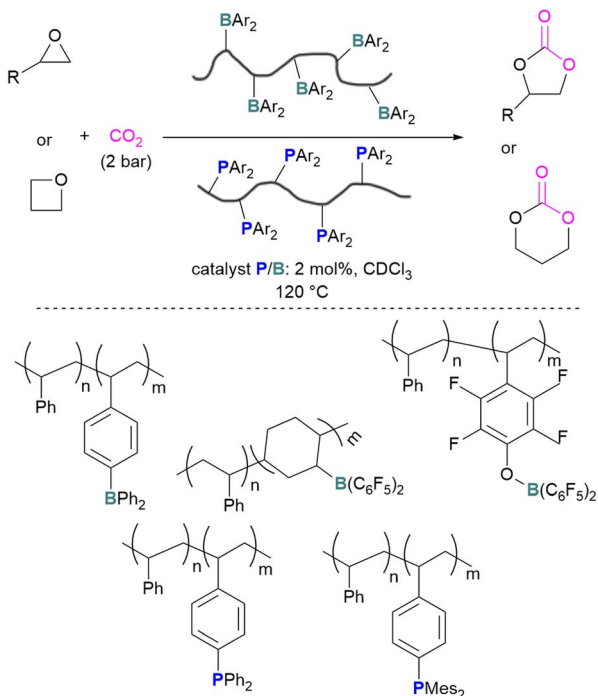


Scheme 18 CO₂-responsive dynamic gel system based on a FLPs.

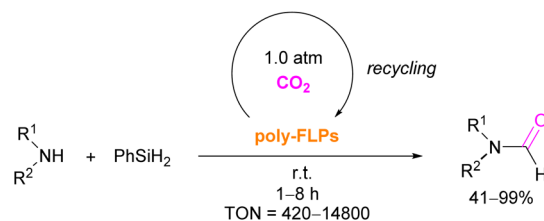
Various amines were screened and the yields for the formamide products were in the range of 41–99% with TON = 420–14 800. The highest TON of 14 800 was observed for diethylamine giving 99% yield of the corresponding diethylformamide product (Scheme 19).⁶³ CO₂ bridges the polymer chains and a CO₂-triggered micellisation was obtained. Addition of PhSiH₃ and R¹R²NH resulted in the desired formamide products and regenerated the polymer. After separation of the products re-micellisation of the polymers was performed with CO₂ and a reusable catalytic system was established with a high turnover number.

Erasmus and co-workers developed efficient FLPs supported on silica nano-powder for CO₂ capture.⁶⁴ A series of CO₂ adducts **28** were synthesised by reacting silica nanopowder supported Lewis acids and dissolved Lewis bases in pentane with CO₂ (2 bar) which was passed through the pentane mixture at -65 °C. At room temperature these adducts were observed to be reversible in nature (Scheme 20, top).

In a similar manner a series of silica nano-powder supported FLP-CO₂ adducts **29** were synthesised from silica nano-powder supported Lewis bases and dissolved Lewis acids. The silica nanopowder supported FLPs were also explored for the conversion of CO₂ to formic acid using hydrogen gas. Initially, the activation of H₂ was done by the supported Lewis acid/bases with FLP partners to obtain [-BH]⁻ [HP-]⁺ salts. Furthermore, introducing CO₂ to these salts resulted in HCO₂H and regenerated the FLPs. HCO₂H is a protic polar molecule and has tendency to form O...H bonds with the free -OH functionalities on the silica. The main reason for the release of HCO₂H from the system after reduction was the immobility of silica nano-powder bound Lewis acids (or Lewis bases) and so did not inhibit the activity of the FLPs.



Scheme 17 Polymeric FLP-catalysed reaction of ethers and CO₂ for cyclic carbonate formation (top), and polymers used (bottom).



Scheme 19 -B-CO₂-P- poly-FLPs in formamide synthesis.



Scheme 20 FLPs supported on silica nano-powder for CO₂ capture.Fig. 6 Structures of N-CO₂-B adducts. PMP = 1,2,2,6,6-Pentamethylpiperidine.

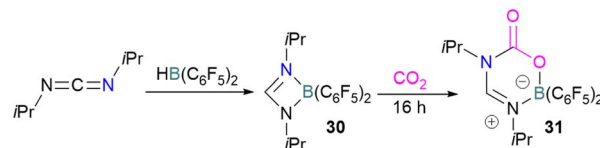
In FLP systems having a P-basic centre, activation of CO₂ proceeds *via* the formation of a P-C bond, and depending on the type of reactive acidic site a B-O, Al-O or Ga-O bonds are generated, often in a reversible manner. Alkyl phosphines *i*Pr₃P or *t*Bu₃P alone could not activate the CO₂ molecule. It is known that the presence of a Lewis acidic component is not necessary for capturing CO₂ when very electron rich P-nucleophiles are used.⁶⁵

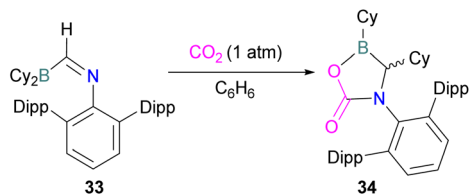
Borane/nitrogen FLPs for CO₂ activation

In addition to phosphorus as a Lewis base in FLP-CO₂ activation and reduction, there has been a wealth of FLPs described in the literature that use a nitrogen Lewis base in combination with a boron Lewis acid. A selection of the corresponding FLP-CO₂ adducts are displayed in Fig. 6.^{66,67}

Stephan and co-workers reported a new synthetic method for making boron amidinates. The strained ring boron amidinate derivative **30** was prepared by reacting Piers' borane, HB(C₆F₅)₂, with isopropyl carbodiimide. **30** was then successfully employed to trap CO₂ incorporated into a new heterocycle **31** (Scheme 21). Compound **31** was fully characterised along with a single crystal X-ray diffraction structure.⁶⁸ A theoretical study on the reaction of **30** with CO₂ found a concerted addition mechanism.

In this reaction, the C-atom and O-atom of CO₂ inserts into the B-N bond of **30** and forms the C-N and B-O bonds simultaneously. The frontier orbitals involved in the reaction mechanism were investigated as well as electric charge analysis and showed that results were consistent with charge transfer from HOMO of **30** to the LUMO of CO₂.⁶⁹ In another findings, Chat-taraj and co-workers have studied this boron amidinate **30** as a bridged B/N FLP.⁷⁰ They compared **30** with a P/B bridged system shown in Scheme 15 which describes two types of cycles. In this work, a similar process shows that CO₂ hydrogenation with amidinate **30** leads to formic acid (HCO₂H) as the final product. In the proposed mechanisms, either H₂ is activated by the Lewis basic centre of the FLP, and CO₂ is activated by the Lewis acidic centre of the FLP, or alternatively, CO₂ can be activated by Lewis basic centre of the FLP and H₂ by Lewis acidic centre of the FLP. In both cases, simultaneous activation of CO₂ and H₂ by a single TS was confirmed by Natural Bond Orbital (NBO) analysis and this TS is the rate determining step. From energy decomposition analysis (EDA), in the TS geometry it was found that electron density was donated from the HOMO of FLP to the LUMO of H₂ and electron density from HOMO of H₂ molecule to the LUMO of CO₂.⁷⁰ Stephan and co-workers have also utilised phosphinimines and B(C₆F₅)₃ to explore FLP reactivity, Ph₃P=NR with B(C₆F₅)₃ and CO₂ produced the adducts **32** (R = Ph, C₆F₅) (Scheme 22).⁷¹ Figueroa and co-workers observed that (boryl)iminomethane **33** reacts

Scheme 21 Synthesis of boron amidinates and reaction with CO₂.Scheme 22 Activation of CO₂ using phosphinimines and B(C₆F₅)₃.



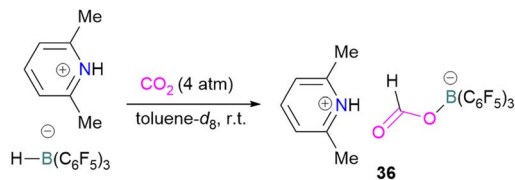
Scheme 23 CO₂ adduct of (boryl)iminomethane. Dipp = 2,6-Diisopropylphenyl.

intramolecularly with CO₂ and forms a five-membered ring **34** in a 1,2-cyclohexyl shift (Scheme 23). Due to the 1,2-cyclohexyl shift, product **34** is stable and prevents the release of CO₂, exhibiting irreversibility. Heating of the solution of **34** to 80 °C showed no release of CO₂. Likewise, heating of the solid sample of **34** to 150 °C under vacuum did not display any CO₂ release either.⁷²

N/B CO₂ adducts have also been used in subsequent stoichiometric transformations. It has been previously reported that TMP [2,2,6,6-(tetramethylpiperidine)] along with B(C₆F₅)₃ splits H₂ heterolytically and forms the ion pair [TMPH][HB(C₆F₅)₃].⁷³ O'Hare and co-workers utilised this ion pair [TMPH][HB(C₆F₅)₃] to insert CO₂ into the B–H bond forming a formatoborate complex **35** at elevated temperatures. Compound **35** can also be obtained from the reaction of TMP, B(C₆F₅)₃ and HCO₂H (Scheme 24). The structure of **35** was confirmed by single crystal X-ray diffraction analysis.⁷⁴ The formatoborate complex **35** could be transformed to produce MeOH by applying more equivalent of ion pair [TMPH][HB(C₆F₅)₃]. The formation of [(C₆F₅)₃B–OH][−] is an obstacle for this method to be developed into a catalytic transformation. A similar FLP system consisting of 2,6-lutidine/B(C₆F₅)₃ has also been shown to split H₂ heterolytically to form borohydride salt [(CH₃)₂C₅H₃NH][HB(C₆F₅)₃].⁷⁵ Mayer and co-workers applied this salt for the activation of CO₂ at 4 atm pressure and at room temperature. The air-stable formatoborate complex **36** (Scheme 25) resulted and its structure was confirmed by X-ray diffraction analysis.⁷⁶ Compared to **35**, Mayer and co-workers observed that **36** on heating to 80 °C resulted only in decomposition instead of transforming to other CO₂ reduced products. This restricts the method to obtain only formatoborate complex **36** in a stoichiometric way. Fontaine and co-workers explored the hydrogenation of carbon dioxide using intramolecular *o*-phenylene bridged B/N FLPs **37** (Scheme 26). When R = 2,4,6-Me₃C₆H₂, the FLP species forms the formyl, acetal and methoxy derivatives **38**, but when R = 2,4,5-Me₃C₆H₂, the boron-linked product **39** formed instead.⁷⁷



Scheme 24 Formation of a formatoborate complex with the TMP/B(C₆F₅)₃ FLP.

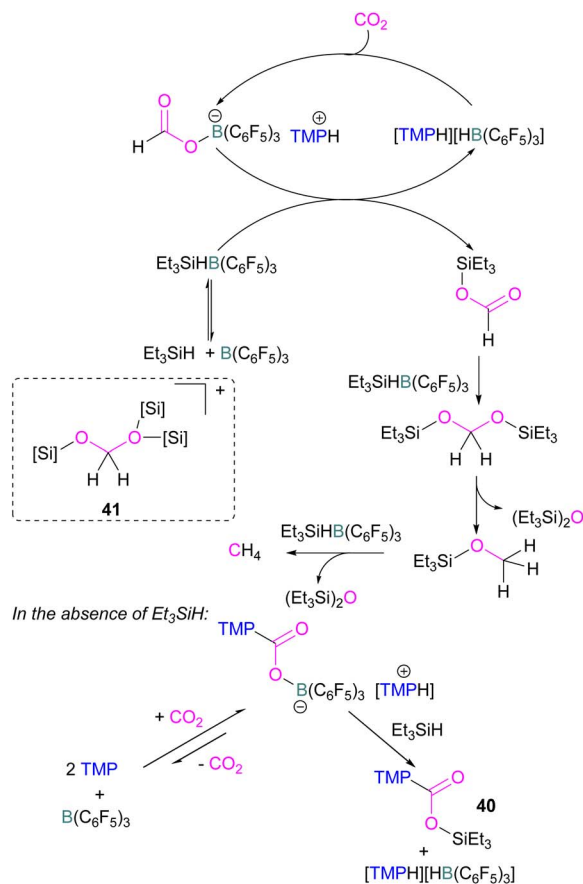


Scheme 25 Formation of a formatoborate complex with the 2,6-lutidine/B(C₆F₅)₃ FLP.



Scheme 26 Hydrogenation of CO₂ using intramolecular B/N FLPs.

Catalytic transformations of CO₂ have also been successful using B/N FLP systems. To address the catalytic shortcomings of the reaction developed by O'Hare and his group using the FLP



Scheme 27 Converting stoichiometric CO₂ reduction into a catalytic process by adding excess B(C₆F₅)₃ and Et₃SiH to the TMP/B(C₆F₅)₃ FLP system.



TMP/B(C₆F₅)₃ for the reduction of CO₂ with H₂ to form methanol, Piers and co-workers developed a catalytic method by adding silane to the reaction mixture with excess B(C₆F₅)₃ to form methane (Scheme 27).⁷⁸ They also reported that when Et₃SiH was not added to the reaction, then the CO₂ adduct as the salt [TMP-CO₂-B(C₆F₅)₃][TMPH] was formed. As seen in other systems, the formation of the CO₂-adduct is reversible, however, when Et₃SiH is added then it provided the [TMPH][HB(C₆F₅)₃] salt along with a triethylsilyl carbamate **40**.⁷⁸

For this reaction, Wang and co-workers carried out computational studies to look at the mechanism of CO₂ reduction to methane with Et₃SiH catalysed by the ion pair [TMPH][HB(C₆F₅)₃] in combination with B(C₆F₅)₃ in detail. The mechanism proposed by Piers was confirmed to be energetically feasible in this study. The reduction proceeds *via* CO₂ insertion into [TMPH][HB(C₆F₅)₃], followed by three successive hydride transfers from Et₃SiH to the CO₂ centre. It was confirmed that the insertion of CO₂ into the H-B bond of [TMPH][HB(C₆F₅)₃] proceeds in a stepwise manner with H^{δ+} and H^{δ-} in the salt first transferring to CO₂ to form **41** (Scheme 27, insert).

The role of B(C₆F₅)₃ was also found to be important since it promotes hydride transfer and acts as a shuttle to bring H^{δ-} from Et₃SiH to CO₂.⁷⁹ Overall, additional B(C₆F₅)₃ activates the silane reducing agent, Et₃SiH, producing Et₃Si⁺ as a good oxygen acceptor and thus promotes the catalytic deoxygenation of CO₂ to CH₄.

Cantat and co-workers explored nitrogen bases such as TBD (triazabicyclodecene), Me-TBD (MTBD), DBU (1,8-diazabicyclo[5.4.0]undec-7-ene), and others for the reduction of CO₂ in the

presence of 9-BBN or CatBH. The reactions were performed at room temperature and a TON of up to 648 was achieved (Scheme 28). In this process, CO₂ is initially reduced to a borlyformate which then undergoes reduction firstly to an acetal and then a methoxyborane. The stoichiometric reaction of TBD-CO₂ and 9-BBN in THF forms product **42** along with other reduced products (Scheme 28). Compound **42** was analysed by single crystal X-ray diffraction and it was found that the acidic NH proton in the TBD-CO₂ adduct was replaced with a 9-BBN unit. Compound **42** can be considered as a nitrogen/boron FLP system trapped with CO₂. A mechanism was proposed based on rigorous control experiments. In **42**, CO₂ behaves as a Lewis base and coordinates to the hydroborane R₂BH to form adduct **43**, which enables hydride transfer from the borane to carbon and forms **44**. Compound **42** is regenerated when CO₂ is applied, releasing the boron formate and thus catalysed the system for CO₂ hydroboration. Finally, the boron formate is reduced to the methoxyborane. It is important to note that for MTBD it was found that the reaction proceeds with the activation of borane followed by the capture of CO₂.⁸⁰

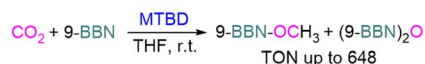
Stephan and co-workers inadvertently discovered a new class of N/B molecule **45**, that consists of a strong Lewis basic phosphorus centre and weak Lewis acidic boron centre which makes it a suitable FLP system. They utilised FLP **45** in the reduction of CO₂ (5 atm) at 60 °C with BH₃·SMe₂ as a reducing agent and obtained a boroxine product (Scheme 29).⁸¹ The reduction of CO₂ was observed catalytically in this case due to the presence of a strong basic centre and a weak Lewis acid that facilitates lability of the reduced CO₂ fragments. This shows a difference to FLPs composed of a strong Lewis acid in which only stoichiometric reduction was observed, as in the case of **18** where 1,2-C₆H₄(BCl₂)₂ is the Lewis acid (Scheme 11).

Zhang *et al.* found that 4 equivalents of BH₃·NMe₃ and catalytic 6-amino-2-picoline could be used to formylate secondary amines. The proposed mechanism proceeds through dehydrocoupling of the amineborane and catalyst to form an intramolecular FLP **46**, which reacts with CO₂. The activated CO₂ is then inserted into the N-B bond which is subsequently reduced by borane with loss of H₂BOBH₂ to give the methylated amine (Scheme 30).⁸²

For the activation of CO₂ using FLPs, many arrangements of plausible Lewis pairs are possible. Hence, it is a challenge to find a particular combination that is superior for catalysing CO₂ reduction.

With this in mind, Corminboeuf and co-workers proposed a map of chemical composition of FLPs for their activity towards

Catalytic CO₂ reduction by MTBD:



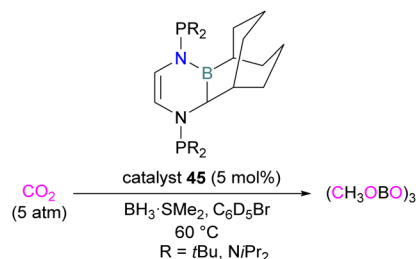
Formation of TBD-CO₂-BBN adduct:



Mechanistic cycle:

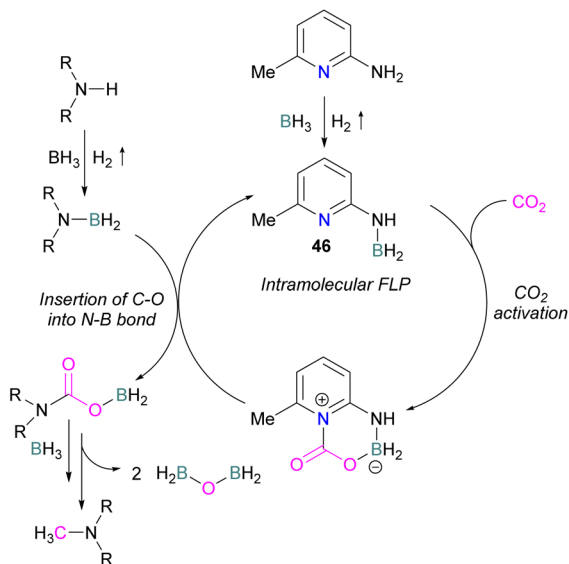


Scheme 28 Catalytic reduction of CO₂ using N-bases and B-H reducing agents.



Scheme 29 Catalytic reduction of CO₂ using FLP **45**.





Scheme 30 Catalytic transformation of CO₂ by *N*-methyl formylation of secondary amines.



Scheme 31 Catalytic transformation of CO₂ to formate using the inverse FLP consisting of tbtb and DBU.

formate product by catalytic hydrogenation of CO₂. They built the map upon linear scaling relationships, pinpointing specific FLP combinations with complementary acidity and basicity to optimally balance the energetics of the catalytic cycle. Amongst such combinations, they created a library of 60 P/N Lewis bases and 64 triaryl boranes as Lewis acids resulting in a library of 3840 FLPs. Out of these, they experimentally demonstrated the catalytic transformation of CO₂ to formate by using an inverse FLP system obtained from tris(*p*-bromo)tridurylborane (tbtb) as Lewis acid and DBU as the Lewis base. A turnover number of 24 ± 3 was found for this catalytic reaction (Scheme 31). This is the first example of a metal-free CO₂ hydrogenation in which stoichiometric addition of a silylhalide was not required. This was achieved through the fine-tuning of the Lewis acid and base based on their energies of hydride and proton attachment, respectively. Here, the authors conclude that inverse FLPs, with a weaker Lewis acid and strong Lewis base or strong Lewis acid with weaker Lewis base, yet with cumulative high acid–base strength, is the ideal combination to achieve CO₂ hydrogenation. The authors highlight the importance of overcoming both



Scheme 32 CO₂ adducts of bis(boramidinate)ferrocenes.

activation barriers to CO₂ activation as well as H₂ activation when targeting catalytic CO₂ hydrogenation.⁸³

In 2022, Palomero and Jones reported the preparation of bis(boramidinate)ferrocenes **47** and **48** by hydroboration of 1,1'-dicarbodiimidoferrrocenes. The resulting compounds reacted with CO₂. The reaction of the BBN derivative **47** with CO₂ (10 atm) to form the mono-CO₂-bound product as a yellow precipitate (90% conversion) in a process that was highly reversible (Scheme 32). Whilst this precluded isolation of the CO₂-bound products, such reversibility may be preferable for applications in catalytic hydrogenation, facilitating release of the reduced product and catalytic turnover. Lower pressures of CO₂ were shown to reduce conversion.⁸⁴ To allow the use of lower pressures, the more electron-poor bis(pentafluorophenyl)borane analogue **48** was employed. At 5 atm CO₂, it activated 2 equivalents of CO₂, although the reaction required two weeks to go to completion.

Borane/carbon FLPs for CO₂ activation

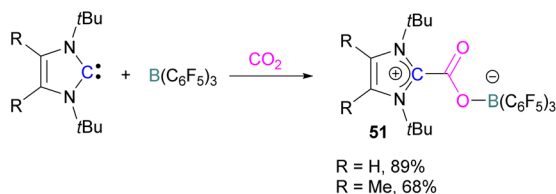
Stable *N*-heterocyclic carbenes (NHCs) upon reaction with CO₂ form a mesomeric betaine **49** having a C–C bond between the



Scheme 33 Reaction of carbenes with CO₂.Scheme 34 First carbene based FLP system for CO₂ activation.

carbene and CO₂. On the other hand, very reactive carbenes can form oxiranones **50** (Scheme 33). The product remains in equilibrium with the starting substrates. Most attention has been focused on stable sterically hindered NHCs amongst all carbenes for the activation of small molecules,⁸⁵ and several carbenes in FLP systems have been explored and found to be efficient in the activation of CO₂.⁸⁶

The first carbene based FLP system to activate CO₂ was reported by Tamm and co-workers in 2012 (Scheme 34).⁸⁷ They showed that exposure of CO₂ to a solution of a bulky carbene (1,3-di-*tert*-butylimidazolin-2-ylidene) and tris[3,5-bis(trifluoromethyl)phenyl]borane, B(3,5-(CF₃)₂C₆H₃)₃, in benzene at 60–70 °C, a white precipitate, identified as the FLP-CO₂ adduct was formed. The adduct was isolated in 66% yield. At room temperature this adduct was also obtained on exposure of CO₂ to the solution of the FLP in benzene with a 24 h reaction time and a higher yield of 86% was isolated.

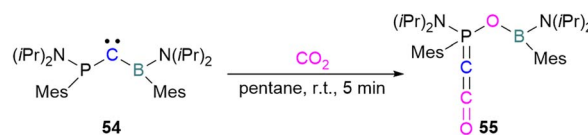
Scheme 35 Capture of CO₂ with NHC/B(C₆F₅)₃ FLPs.

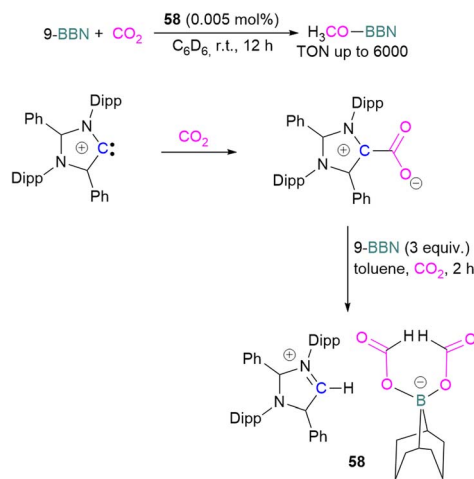
Scheme 36 Computationally designed carbene/borane derived FLP.

Later, Tamm and his group synthesised a library of carbene based FLP CO₂-adducts and studied their reaction profile computationally (level of theory: M05-2X/6-311G**). A 1:1 mixture of a bulky carbene and B(C₆F₅)₃ with CO₂ provided NHC-CO₂-B(C₆F₅)₃ products **51** in 89% and 68% yield depending on the starting carbene (Scheme 35). From DFT calculations a low energy barrier was observed for the NHC-CO₂-B(C₆F₅)₃ adduct formation (10.4 (R = H) and 12.2 (R = Me) kcal mol⁻¹), and it was concluded that steric changes on the NHC were more pronounced than electronic impacts.⁸⁸

Zhu and co-workers computationally designed a boron-based carbene intramolecular FLP **52** and calculated its reactivity with various small molecules, including CO₂. This FLP with CO₂ forms a zwitterionic species **53** and the authors discuss the important driving force of aromaticity in the final adduct (Scheme 36).⁸⁹ Baceiredo and co-workers exposed boryl(phosphine)carbene **54** to CO₂ (1 atm) and an unusual product **55** was observed. After analysis of the product's structure, it was found that the carbene inserted into the C=O bond of the CO₂. Thus, incorporating carbon dioxide into the corresponding phosphoryl ketenylidene derivative (Scheme 37).⁹⁰

Stoichiometric reduction reactions with carbene/borane FLPs have been reported.⁹¹ In 2019, Mandal and co-workers prepared an *N*-heterocyclic carbene-boron adduct **56** by reacting an abnormal heterocyclic carbene (aNHC) with 9-BBN. The synthesised NHC-boron adduct **56** was utilised to capture CO₂ from the atmosphere under ambient conditions in benzene overnight. Product **57** was obtained, due to moisture in the air

Scheme 37 CO₂ adduct of a boryl(phosphine)carbene.Scheme 38 NHC-BBN adduct captures CO₂ from the air under ambient conditions and reduction to formate and methoxide.



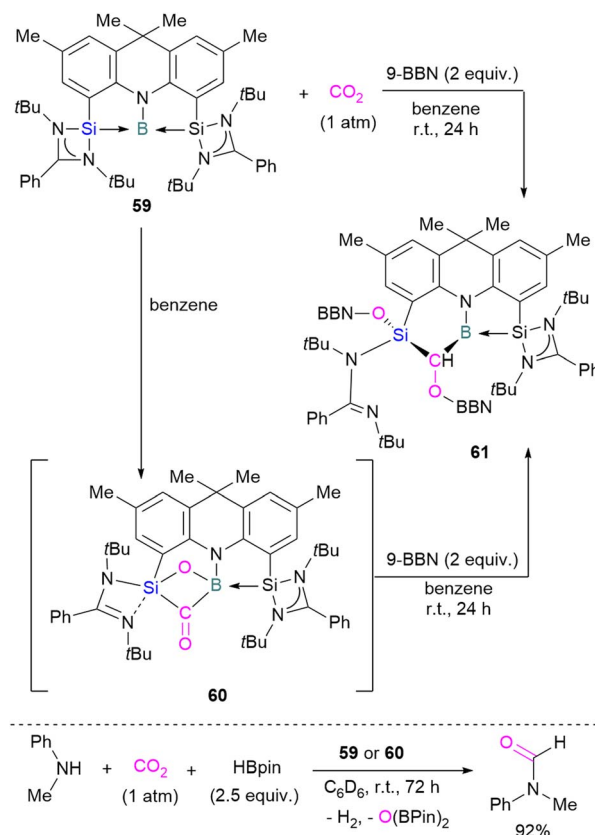
Scheme 39 Preparation of zwitterionic boron diformate **58** and its use as a catalyst for the reduction of CO₂.

leading to hydrolysis of 9-BBN and boric acid formation with the release of a cyclooctane molecule. The CO₂ was incorporated as a formate ion. Further treatment of **57** with excess 9-BBN leads to the formation of compound CH₂(OBBN)₂ with the release of H₂, and finally converts this to CH₃OBBN (Scheme 38).⁹¹ This work was presented as a first metal-free system to reduce CO₂ by capturing it from the atmosphere under ambient conditions where CO₂ remains in a concentration of ~400 ppm. Mandal and co-workers later reported the use of the same FLP system for a catalytic reduction of CO₂ in the presence of a range of hydroboranes leading to methoxyborane (Scheme 39). Reaction of the carbene with CO₂ firstly gave the adduct whilst reaction of the carbene with 3 equivalents of 9-BBN in the presence of CO₂, provided boron diformate **58**. Zwitterionic boron diformate **58** was utilised catalytically with a loading of 0.005 mol% for the conversion of 9-BBN to the methoxide derivative CH₃O-BBN under a CO₂ atmosphere. Catalyst **58** leads to a TON of 6000, which is the highest TON observed among all the metal-free catalysts investigated at ambient conditions. The key feature of this catalytic process is the formation two equivalents of 9-BBN formate, BBN(OCHO), from the reaction of catalyst **58** with an equivalent of 9-BBN resulting in the release of dihydrogen.

This generates the carbene which further captures a CO₂ molecule regenerating **58** with 9-BBN and thus providing a catalytic process. The 9-BBN formate is finally reduced and hydroborated to CH₃O-B in a series of steps in the presence of an excess of 9-BBN.⁹²

Borane/silicon FLPs for CO₂ activation

To date there is just one example of a boron/silicon FLP for CO₂ activation. Very recently Mo and co-workers reported the synthesis of a geometrically constrained bis(silylene)-stabilised borylene **59**.⁹³ Spectroscopic and X-ray analyses reveal that structure **59** has a tricoordinate boron centre with a distorted T-shaped geometry. Computational analysis shows that the HOMO comprises a lone pair of electrons on the boron centre



Scheme 40 Cooperative bond activation of CO₂ with a borylene/silylene compound and catalytic application.

and is delocalised over the Si–B–Si unit. Compound **59** shows single electron transfer reactivity towards B(C₆F₅)₃ forming a frustrated radical pair [(SiNSi)B]^{•+}[B(C₆F₅)₃]^{•-}. The reaction of **59** with CO₂ (1 atm) in C₆D₆ at room temperature forms a new product **60** by cleaving CO₂ which, upon hydroboration with two equivalent of 9-BBN, forms compound **61** in quantitative yields. The structure of **61** showed that boron and silicon atoms are bridged by boryloxymethylene (CHOBR₂) formed by the hydroboration of the C=O group. The Si–O–B bridge in **60** was cleaved along with the formation of BH and SiOBR₂ units. Compound **61** can also be obtained directly by treating **59** with CO₂ and 2 equivalents of 9-BBN in C₆D₆ at room temperature with an isolated yield of 45% (Scheme 40). The catalytic performance of **59** (5 mol%) and **60** (5 mol%) shows an efficient transformation of *N*-methylaniline into the corresponding formamide (92% yields in each case) by capturing and hydroborating CO₂ with HBpin (Scheme 40).⁹³

Borane/germanium FLPs for CO₂ activation

Similar to the silylene described above, germynes are also reported as the Lewis base component of an FLP for CO₂ reduction. Kato and co-workers reported an interesting *N,P*-heterocyclic germylene **62** in 2016, that bears several reactive sites (including a germylene centre) and can activate two CO₂ molecules simultaneously.⁹⁴ Compared to classical FLPs, **62** showed unusual behaviour of multi-reactive sites and has been



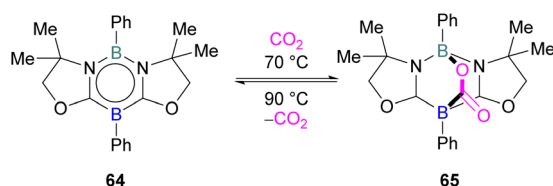


Scheme 41 *N,P*-heterocyclic germylene in catalytic hydrosilylation of CO₂.

utilised as a donor component in the Lewis acid–base pair. In fluorobenzene, the *N,P*-heterocyclic germylene **62** reacts with B(C₆F₅)₃ at room temperature to give the corresponding adduct **62**·B(C₆F₅)₃ as colourless crystals in 67% yield (Scheme 41). The authors explored the catalytic reduction of CO₂ with 5 mol% of the FLP adduct **62**·B(C₆F₅)₃ and the reducing agent Et₃SiH. The proposed mechanism for CO₂ activation showed that **62**·B(C₆F₅)₃ reacts with silane Et₃SiH and forms a cationic germylene **63** which promotes CO₂ hydrosilylation catalytically *via* two possible activation modes **A** and **B** to obtain product H₂-C(OSiEt₃)₂ selectively.⁹⁴

Borane/boron FLPs for CO₂ activation

FLP systems where the same element is used both as the Lewis acidic and Lewis basic reactive centres are rarely observed. One such example was reported by Kinjo and co-workers in 2015



Scheme 42 Reaction of a 1,3,2,5-diazadiborinine with CO₂.

with 1,3,2,5-diazadiborinine **64** featuring nucleophilic and electrophilic boron centres within the same molecule.⁹⁵

This first reported intramolecular boron–boron FLP showed high regioselectivity in the reaction with CO₂, yielding a bicyclic product **65** (Scheme 42). Interestingly, CO₂ activation by **64** was reversible at 90 °C. To obtain insight into electronic features of 1,3,2,5-diazadiborinine **64**, the authors performed DFT calculations [level of theory: B3LYP/6-311G+(d,p)]. NBO analysis showed that the compound possess both nucleophilic and electrophilic boron centres with a formal B(+I)/B(+III) mixed valence system.⁹⁵ Later, Zhao and co-workers performed more detailed computational analyses of **64**.⁹⁶ They reported π delocalisation over the central ring which extends from the lone pair on (O) $\rightarrow \pi^*(N-C)$, and favourable orbital overlap with CO₂ is generated from the electrophilic interaction with the Lewis acidic boron centre and nucleophilic donation to the LUMO+3 of the other boron centre.

Kinjo and co-workers synthesised another class of boron compounds in which the boron acts as a Lewis basic centre.

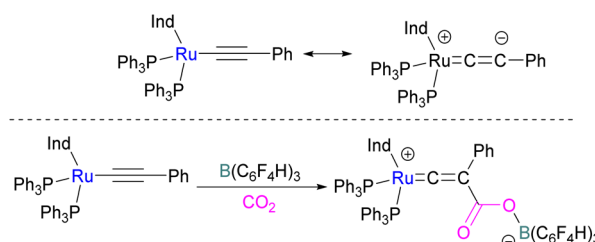
It was found previously that tricoordinate organoboron L₂PhB: (L = oxazol-2-ylidene) compound **66** does not react with BEt₃. This is perhaps due to a mismatch of the softness/hardness of the respective boron centres in **66** and BEt₃ based on HSAB (Hard Soft Acid Base) theory in addition to steric hindrance. As compound **66** and BEt₃ do not react, they act like an FLP. Thus **66** and BEt₃ were reacted with CO₂ in toluene at room temperature and the FLP-CO₂ adduct was isolated in 85% yield (Scheme 43).⁹⁷

Borane/metal FLPs for CO₂ activation

In addition to p-block Lewis bases, transition metal complexes can also act as the Lewis base component of an FLP with boron as the Lewis acid. This is demonstrated using a ruthenium



Scheme 43 Reaction of tricoordinate organoboron compound with Et₃B and CO₂.



Scheme 44 CO₂ adduct of [(η^5 -indenyl)Ru(PPh₃)₂(CCPh)] and B(C₆F₄H)₃. Ind = Indenyl.





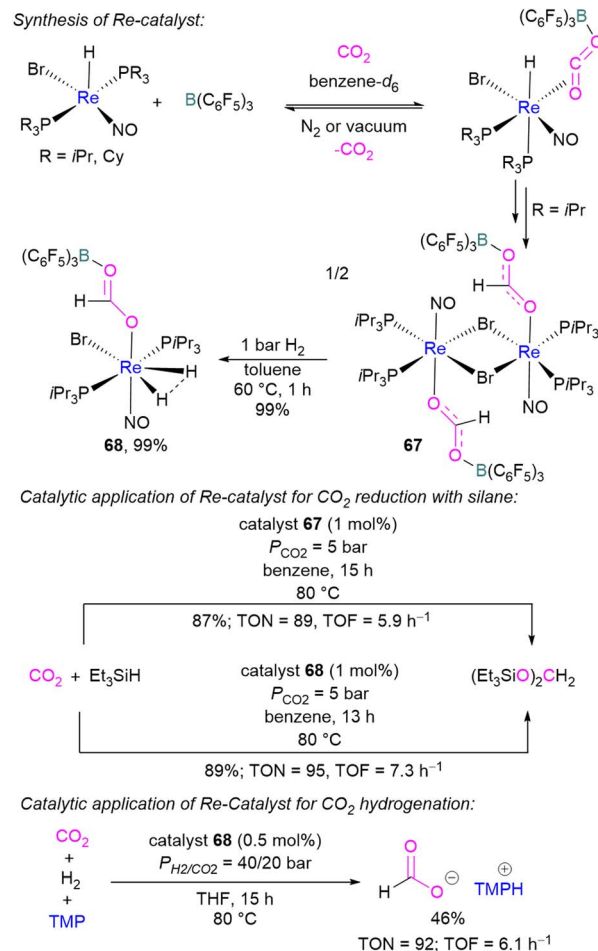
Scheme 45 Activation of CO₂ using Lewis basic platinum(0)-CO complex/B(C₆F₅)₃.

acetylide which is an electron rich species. This can create a Lewis basic β -carbon centre and form an FLP when combined with a Lewis acid (Scheme 44). Stephan and co-workers in 2013 showed that when $[(\eta^5\text{-indenyl})\text{Ru}(\text{PPh}_3)_2(\text{CPh})]$ was reacted with $\text{B}(p\text{-C}_6\text{F}_4\text{H})_3$ no reactivity was observed, indicating that their combination is an FLP in nature. A solution of this FLP, when exposed to CO₂ for 12 h, provided an orange solid in 70% yield and was fully characterised using NMR and single crystal X-ray crystallography as the FLP-CO₂ adduct where the β -carbon centre had attacked the electrophilic carbon centre of CO₂ (Scheme 44).⁹⁸

Wass and co-workers explored reactions with a platinum(0) complex as a Lewis base in the activation of small molecules using a sterically congested boron-based Lewis acid. They found that pairing a Lewis basic platinum(0)-CO complex supported by a diphosphine ligand with $\text{B}(\text{C}_6\text{F}_5)_3$ acts as a frustrated Lewis pair, to activate CO₂ (Scheme 45). The presence of $\text{B}(\text{C}_6\text{F}_5)_3$ is important as no activity was observed between the platinum complex and CO₂ in the absence of the borane. In this scenario, Pt(0) acts as a donor of electron and the boron atom acts as the acceptor forming a coordinated Pt-CO₂-B system. A substitution of CO by CO₂ on platinum was observed after the loss of the CO molecule.

In this process 95% isotopically pure ¹³CO₂ was used but the ³¹P NMR analysis of the product showed a mixture of ¹³C labelled and unlabelled product in a ratio of 4 : 1. The source of unlabelled product must be from the ¹²CO in ligand of the starting material. This suggests that a symmetrical $[\text{C}_2\text{O}_3]^{2-}$ complex forms during the reaction pathway. The proposed mechanism in Scheme 45 suggests that the reaction of the platinum(0)-CO complex and $\text{B}(\text{C}_6\text{F}_5)_3$ with CO₂ is a metal-mediated oxygen transfer between CO₂ and CO rather than a simple ligand substitution.⁹⁹

In 2013, Berke and co-workers showed an FLP-type activation of CO₂ using a $[\text{Re}]\text{-H}/\text{B}(\text{C}_6\text{F}_5)_3$ system where the Re-H bond acts as a Lewis base. Catalysts **67** and **68** were prepared stepwise from a rhenium hydride precursor $[\text{ReH}(\text{PR}_3)_2(\text{NO})\text{Br}]$ (Scheme 46). Initially, the precursor was reacted with $\text{B}(\text{C}_6\text{F}_5)_3$ and CO₂ in benzene to form the FLP-CO₂ adduct. With a $\text{P}i\text{Pr}_3$ ligand on the rhenium precursor, insertion of the Re-H into the FLP-bound CO₂ molecule was observed generating **67**. Compound **67** could be hydrogenated with H₂ (1 bar) in toluene at 60 °C for 1 h

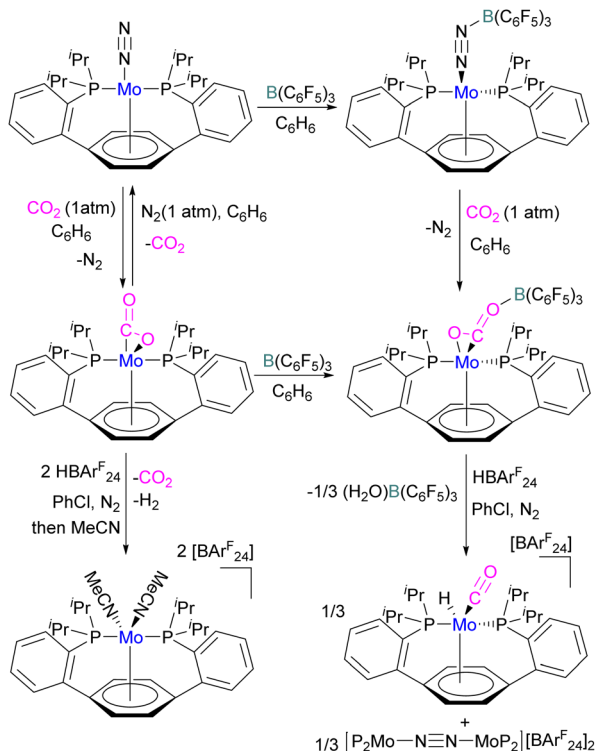


Scheme 46 Synthesis of $[\text{Re}]\text{-CO}_2\text{-B}(\text{C}_6\text{F}_5)_3$ adduct and utilisation as a catalyst in CO₂ reduction.

to give **68** in 99% yield. Both **67** and **68** were screened for the hydrosilylation of CO₂ using Et_3SiH as a reducing agent (Scheme 46). Catalyst **67** with a loading of 1 mol% provided the $(\text{Et}_3\text{SiO})_2\text{CH}_2$ product in 87% yield ($\text{TON} = 89$, $\text{TOF} = 5.9 \text{ h}^{-1}$), while **68** provided the reduced product in 89% yield ($\text{TON} = 95$, $\text{TOF} = 7.3 \text{ h}^{-1}$). Similarly, catalysts **67** and **68** were utilised for CO₂ hydrogenation ($P_{\text{H}_2/\text{CO}_2} = 40/20 \text{ bar}$) in the presence of TMP as a base. Catalyst **68** provided the formate salt of TMP in 46% yield ($\text{TON} = 92$, $\text{TOF} = 6.1 \text{ h}^{-1}$).¹⁰⁰

In another study, Agapie and co-workers investigated the effects of the Lewis acid $\text{B}(\text{C}_6\text{F}_5)_3$ towards the conversion of CO₂ to CO and water using a molybdenum complex (Scheme 47).¹⁰¹ The activation of CO₂ was found to be linearly related to the strength of the Lewis acid. When a labile Mo(0)-CO₂ adduct interacts, it will increase both the degree of activation and the kinetic stability of bound CO₂ as shown in Scheme 47. In contrast to the CO₂ displacement by a solvent that is predominantly observed in the absence of a Lewis acid, in the presence of $\text{B}(\text{C}_6\text{F}_5)_3$ and $[\text{H}(\text{Et}_2\text{O})_2][\text{BAR}^{\text{F}}_{24}]$ ($\text{BAR}^{\text{F}}_{24} = \text{tetrakis}[3,5\text{-bis}(\text{trifluoromethyl})\text{phenyl}]\text{borate}$) CO₂ cleavage occurs. This demonstrates the significance of kinetic and thermodynamic aspects in the effective CO₂ reduction





Scheme 47 Mo based FLP for CO₂ activation. BARF₂₄ = tetrakis(3,5-bis(trifluoromethyl)phenyl)borate.

chemistry primarily relying upon bond activation and the residence period of the associated small molecule.

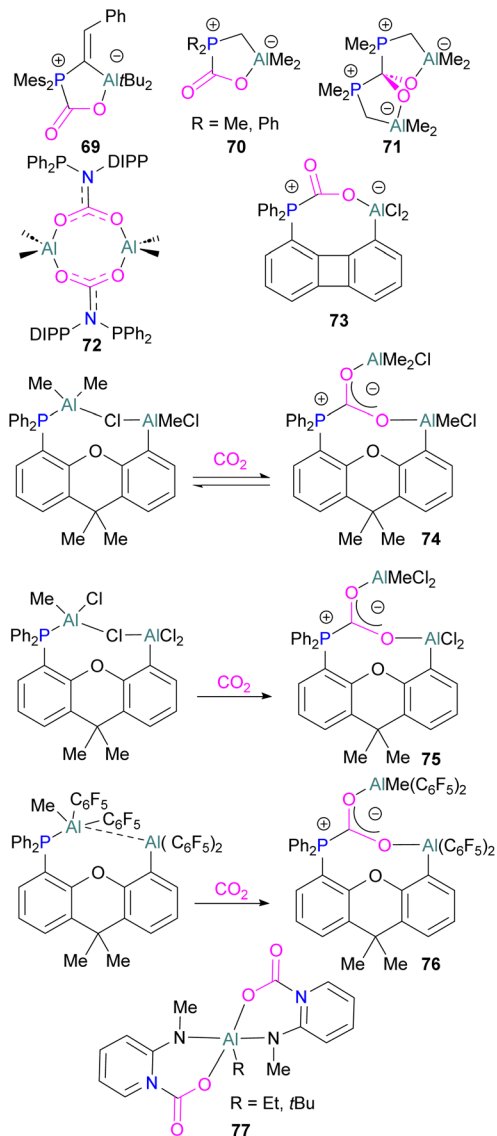
The authors demonstrated that the chemistry of the labile substrate is greatly influenced by the time the substrate resides in the metal's coordination sphere. It is shown that Lewis acid additives promote CO₂ cleavage *via* kinetic stabilisation rather than merely by thermodynamic activation.

One final system to note here uses the boron Lewis acid B(C₆F₅)₃ with s-block metal carbonates M₂CO₃ (M = Na, K, and Cs) for the highly efficient reduction of CO₂ to formate. Amongst the screened metal carbonates, Cs₂CO₃ showed the highest TON of 3941.¹⁰²

Aluminium FLPs for CO₂ activation

A number of FLPs based on aluminium Lewis acids have also been reported for CO₂ capture and reduction, although the greater oxophilicity of aluminium (potentially inhibiting product release) means that catalytic hydrogenation has yet to be reported. This oxophilicity also means that, whereas FLPs containing boron Lewis acids typically bind CO₂ in a 1 : 1 : 1 Lewis acid : Lewis base : CO₂ ratio, Al-containing FLPs often bind it in a 2 : 1 : 1 ratio, with both oxygen atoms binding an aluminium centre.¹⁰³ Studying FLPs comprised of phosphines and aluminium esters, Smythe *et al.*, showed that the ratio of mono- to bis-bound adduct varies with Lewis acidity.¹⁰⁴

After exposure to 1 atm of CO₂, Al(O-C₆H₄Cl)₃ bound CO₂ in a predominantly mono fashion (*ca.* 95% mono), whereas the

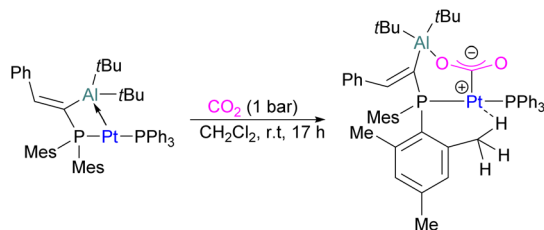


Scheme 48 Aluminium based CO₂ adducts.

greater Lewis acidity of Al(OC₆Cl₅)₃ (*ca.* 1 : 1 mono : bis) and Al(OC₆F₅)₃ (*ca.* 75% bis) favoured the bis-bound adduct.

Like boron CO₂ adducts, a range of aluminium FLP-CO₂ adducts are reported (Scheme 48). Uhl and co-workers reported the synthesis of geminal ambiphilic phosphine-aluminium FLPs that can activate CO₂ to form a cyclic adduct **69**.¹⁰⁵ Later, the same authors synthesised AlPC₂O type heterocycle having *cis/trans* isomeric compounds.¹⁰⁶ Uhl also reported a P-H functionalised Al/P FLP in 2019. The FLP reacts with CO₂ to give a five-membered zwitterionic cycle similar to that in **69**, as typical for vicinal intramolecular FLPs. However, the enhanced acidity of the phosphine means that it can be deprotonated by addition of a base (such as DABCO or *n*BuLi) to give a more stable precipitate.¹⁰⁷ Similarly, Fontaine and co-workers studied the reactivity of the stable Lewis adducts [R₂PCH₂AlMe₂] (R = Me, Ph) and found adducts **70** and **71**.¹⁰⁸ Harder and co-workers reported a geminal Al/P FLP, with a nitrogen rather than the



Scheme 49 Pt/Al bimetallic FLP system in CO₂ activation.

more common carbon linker. Like the carbon-linked Al/P FLP reported earlier by Fontaine, this reacts with CO₂ to give a 2 : 2 eight-membered ring product **72** by insertion of CO₂ into the Al-linker bond with *cis*- and *trans*-isomers.¹⁰⁹ Limberg *et al.* utilised a biphenylene backbone to prepare a strained intramolecular P/Al-based FLP which was reacted with CO₂ (2 bar) at room temperature for 5 minutes in deuterated dichloromethane to obtain adduct **73**.¹¹⁰ They also reported xanthene-linked intramolecular Al/P FLPs containing two Al centres which are able to activate CO₂.¹¹¹

In the products **74–76**, the two aluminium centres each bind to one of the CO₂'s oxygen atoms. The binding strength could be tuned by varying the substituents on aluminium. The more Lewis acidic xanthene-AlCl₂ and xanthene-Al(C₆F₅)₂ fragments bind CO₂ irreversibly giving **75** and **76** (Scheme 48), while xanthene-MeClAl binds CO₂ reversibly giving **74** under 2 bar CO₂, liberating CO₂ when this excess pressure was released. For catalytic applications, this reversible binding is necessary to enable release of the product. Although most CO₂-binding Al FLPs are Al/P rather than Al/N, one example of an Al/N FLP was described by Brewster in 2020 using the readily available 2-(methylamino)pyridine as ligand yielding **77** upon reaction with 2 equivalents of CO₂.¹¹² An example of an FLP-CO₂ adduct with a metal as a Lewis base was provided by Bourissou and co-workers who utilised geminal P-Al ligand [Mes₂PC(=CHPh)Al*t*Bu₂/Pt(PPh₃)] in the activation of CO₂ molecule to obtain an adduct.

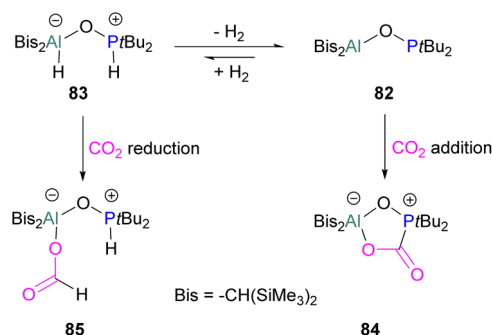
In this bimetallic system, platinum acts as the Lewis base and activates the CO₂ molecule by reacting at the carbon centre of the CO₂ molecule and the formed negative charge on one of the oxygen atoms is stabilised by the Lewis acidic aluminium centre (Scheme 49).¹¹³

Several of these adducts have been used in stoichiometric and catalytic transformations of CO₂. Stephan and co-workers, reported the synthesis of CO₂ adducts **78** between AlX₃ (X = Cl, Br) and PR₃ (R = Mes) (Fig. 7). Upon treatment of these adducts with excess ammonia borane (NH₃·BH₃), an Al-methoxy species was

Fig. 7 Aluminium based FLPs-CO₂ adducts used in CO₂ reduction.Scheme 50 Aluminium based FLP for the stoichiometric reduction of CO₂.

generated which after hydrolysis resulted in the formation of MeOH at room temperature.¹⁰³ To study the steps involved in the reaction, Me₃N·BH₃ was utilised to reduce the FLP-CO₂ adduct **78** (X = C₆F₅, R = *o*-Tol). Along with the methoxy derivatives of alane, compound **79** was isolated and fully characterised.¹¹⁴ Later, other groups have studied the mechanism for this reaction computationally and explained the reduction of CO₂ trapped FLPs.¹¹⁵ In other reactions, Stephan and co-workers explored the adducts of **78** (X = Cl, Br, I, C₆F₅, OC(CF₃)₃ and R = Mes, *o*-tolyl) for the stoichiometric transformation of CO₂ to CO.¹¹⁶

While fluorination of substituents is a common way to increase Lewis acidity in FLP design, an alternative is the use of a cationic Lewis acid. Harder reported an FLP comprised of Lewis basic PPh₃ and a cationic [Dipp-NacNacAlMe]⁺ (NacNac = β-diketiminato ligand) Lewis acid **80**.¹¹⁷ Exposure of this FLP to CO₂ results in the rapid formation of a stable adduct which upon stoichiometric hydrosilylation with triethylsilane forms compound **81** (Scheme 50). Hydride transfer from Et₃SiH to the carbon atom of CO₂ generates Et₃Si⁺ which is trapped by the base, PPh₃, and forms an ion pair [Et₃SiPPh₃]⁺[B(C₆F₅)₄]⁻. The insertion of Et₃Si⁺ into an ion pair restricts the system to stoichiometric CO₂ reduction. Otherwise, cleavage of the Al–O bond and transfer of formate ion HCO₂⁻ to Et₃Si⁺ would have made the system catalytic.

Scheme 51 Oxygen-bridged geminal Al/P FLP for CO₂ activation and reduction.

An unusual report of an oxygen-bridged geminal Al/P FLP **82** was made by Wickemeyer *et al.* (Scheme 51). It was prepared by reaction of the parent alane and phosphine oxide, giving an initial zwitterionic compound **83** which slowly eliminates H₂ to give the FLP **82**. **82** was found to bind CO₂ to give the heterocyclic CO₂ adduct **84**. The hydrogenated zwitterion **83** can also be generated in small quantities by exposure of the FLP to H₂. This species bound CO₂ irreversibly, and exposure of the hydrogen adduct to CO₂ gave stoichiometric CO₂ reduction to the aluminium bound formate **85**.

However, the instability of the hydrogen adduct and strong Al–O bond make the system not well suited for catalytic applications (Scheme 51).¹¹⁸

Huang *et al.* reported a variety of group 12 and group 13 formamidinate FLPs. While formamidinates are able to coordinate as bidentate ligands, the incorporation of strongly electron-withdrawing C₆F₅ substituents on nitrogen increases the preference of the monodentate species with a vacant coordination site on the metal. The free “N” and unsaturated metal in proximity are able to act as an FLP,¹¹⁹ and the compounds' potential for catalytic CO₂ hydrosilylation. While the formamidinates investigated (B, Al, Ga, In and Zn) showed poor activity for this reaction on their own, significantly improved performance was seen when combined with B(C₆F₅)₃ or Al(C₆F₅)₃. The highest activity for complete conversion of triethylsilane under 1 bar CO₂ after 10 h at 80 °C was observed with the aluminium formamidinate/B(C₆F₅)₃, yielding almost exclusively CH₄. Replacing Et₃SiH with Ph₂SiH₂ gave selective formation of the bis(silyl ether).

However, mechanistic studies involving the aluminium formamidinate suggest that the catalyst decomposes under the reaction conditions to generate other aluminium species, which were the catalytically active species, and were not identified.

Surawatanawong and co-workers compared the reactivity of geminal P/Al and B/P FLPs with CO₂ and H₂ based on systems previously published by Lammertsma *et al.*⁴² The compounds investigated consisted of an sp²-carbon bridged FLP (Mes₂P–C(=CHPh)–EtBu₂) and an sp³-carbon bridged FLP (tBu₂P–CH₂–EPh₂) (E = B, Al). In their comparative study between the geminal B/P and Al/P FLP activation of CO₂ and H₂ (Scheme 52), the main conclusions the authors drew are that the FLPs are more reactive towards CO₂ than H₂, and that the geminal B/P



Scheme 52 Geminal P/B and P/Al FLPs with CO₂.

Tandem reduction of CO₂ with a mixed Al/B catalyst:



Mechanism:



Scheme 53 Catalytic reduction of CO₂ by mixed Lewis acids [Al(C₆F₅)₃ and B(C₆F₅)₃]. [B] = B(C₆F₅)₃; [Al] = Al(C₆F₅)₃; [Si] = SiEt₃.

FLPs involve stronger orbital interactions with CO₂ than their Al/P counterparts. Distortion–interaction decomposition showed that the distortion energy in the H₂ fragment is higher than that in the CO₂ transition state leading to a higher energy barrier for H₂ activation than CO₂ activation. This again highlights the importance of considering energy barriers to the activation of both CO₂ and H₂, similarly highlighted by the work of Corminboeuf above (Scheme 31). The type of geminal linker, sp² or sp³, was found not to affect the reactivity.¹²⁰

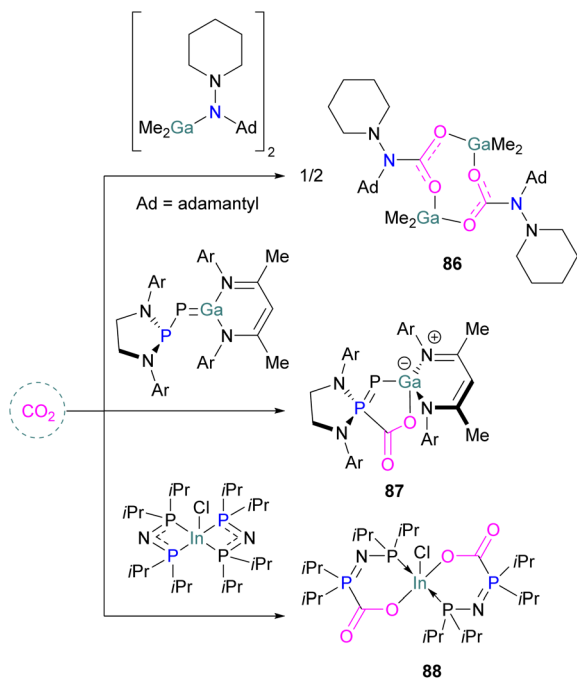
Base-free CO₂ reduction with group 13 Lewis acids

In the final example using only Group 13 Lewis acids, without a base, Chen and co-workers reported the first example of a mixed Lewis acid system consisting of Al(C₆F₅)₃ and B(C₆F₅)₃ for the highly selective reduction of CO₂ into CH₄ via a tandem hydrosilylation (Scheme 53). The reaction proceeds in a catalytic manner. In the first step, Al(C₆F₅)₃ effectively mediates the overall hydrosilylation cycle fixing CO₂ into HCO₂SiEt₃ by activating the carbonyl group. For this initial transformation B(C₆F₅)₃ was found to be inefficient but for the subsequent reduction steps to CH₄ (Scheme 53, steps 2–4) B(C₆F₅)₃ was found to be crucial to give CH₄ in up to 94% yield through a frustrated Lewis pair (FLP)-type Si–H activation. The higher Lewis acidity of Al(C₆F₅)₃ relative to the corresponding borane led to the formation of stable intermediates ([Al]-substrate adducts and [Al]-intermediates). In this reaction for the overall reduction of CO₂ to CH₄, the role observed for both Lewis acids are not only complementary but also synergic where the first reduction step is initiated by the aluminium catalyst and later by the boron catalyst.¹²¹

Gallium and indium FLPs for CO₂ activation

Examples of homogenous gallium and indium containing FLPs in CO₂ activation are rare although several heterogenous





Scheme 54 FLP type reactivity of homogenous indium and gallium systems with CO₂.

systems are known for indium (see later). Uhl and co-workers reported a dimeric gallium hydrazide displaying FLP-like reactivity able to insert CO₂ into the Ga–N bond, yielding a seven-membered C₂O₄Ga₂ cycle **86** (Scheme 54, top).¹²² An atypical example of FLP-like reactivity with CO₂ was also reported by Goicoechea using a phosphanyl phosphagallane.

The compound adds to CO₂ with oxidation of the phosphanyl phosphorus, with gallium bound to the phosphanyl phosphorus and one of the oxygen atoms bound to gallium **87** (Scheme 54, middle).¹²³ Kemp and co-workers prepared a *P,P*-chelated heteroleptic complex bis[bis-(diisopropylphosphino)amido]indium chloride [(iPr₂P)₂N]₂InCl. In both the solid-state and solution, it was found that CO₂ inserted into two of the four M–P bonds to produce [O₂CP(iPr₂)NP(iPr₂)₂]₂InCl **88** (Scheme 54, bottom). Experimental analysis showed that the time taken for the insertion of CO₂ at room temperature in solution condition was less than 1 minute and less than 2 h in the solid–gas reaction. The complex was stable up to 60 °C under vacuum but released CO₂ when heated above 75 °C.¹²⁴

Group 14 Lewis acids

Compared to group 13, group 14 elements have been less studied as Lewis acid components of FLPs for CO₂ activation and conversion. Although carbenium ions such as trityl are isoelectronic with boron, the activation of CO₂ with carbon Lewis acids within an FLP are not known to the best of our knowledge. Examples with heavier Group 14 Lewis acids are known, however, and are described below.



Fig. 8 Si-based CO₂ adducts.

Silicon FLPs for CO₂ activation

Silicon cations are highly electrophilic and are therefore good candidates as the Lewis acid component of FLPs for small molecules activation. In addition, CO₂ transformation into products such as benzoic acid, formic acid, and methanol using silicon cations formed from a [Ph₃C][B(C₆F₅)₄]/R₃SiH system in different solvents has already been shown to be effective.¹²⁵

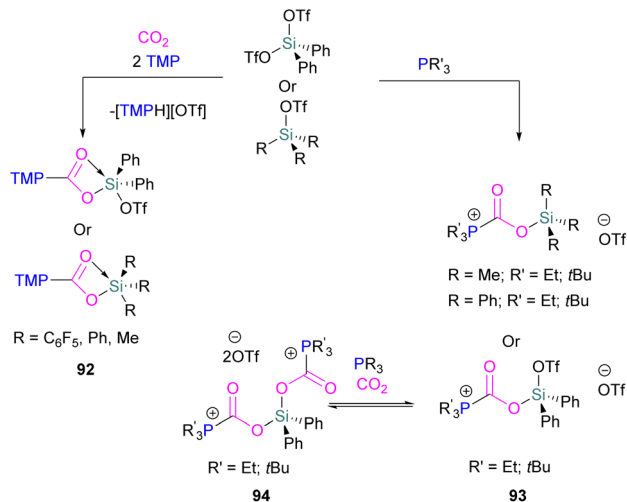
With sterically hindered phosphines, triarylsilylium borates [Ar₃Si⁺][B(C₆F₅)₄] form FLPs. Müller and co-workers studied a series of silylium ion/phosphane Lewis pairs [Ar₃Si⁺/PR₃]. When Ar = Me₅C₆ and R = *t*Bu or Cy these FLPs were able to activate CO₂ (1 atm, 30 min) in benzene at room temperature to obtain the FLP-CO₂ adducts [R₃P–CO₂–SiAr₃] (Fig. 8).¹²⁶ In 2015, Mitzel and co-workers reported the first synthesis of a neutral Si/P FLP (C₂F₅)₃–SiCH₂P*t*Bu₂ and this was utilised in trapping CO₂ at room temperature as a cyclic adduct **89** in quantitative yields.¹²⁷

The stability of the adduct of a trimethylsilylium and a congested *N*-heterocyclic carbene (**90**) was found to be strongly dependent on the nature of the counterion used in the reaction. The stability was found to increase with decreasing nucleophilicity of the ion X, or increasing Lewis acidity of the silylating agent Me₃SiX (X = I, OTf, NTF₂; Tf = SO₂CF₃).¹²⁸ Tamm and co-workers explored the *N*-heterocyclic carbene-silylium ion frustrated FLP for the synthesis of adduct **90** (Fig. 8).¹²⁹

Like the N/B intramolecular FLP described earlier, Cantat and co-workers synthesised a series of TBDR₂SiX [R = Me, *i*Pr, Ph; X = Cl, B(C₆F₅)₄, I; TBD = triazabicyclodecene] compounds and utilised them for CO₂ capture to obtain N/Si⁺ FLP-CO₂ adducts **91** (Fig. 8). The formation and stability of the adducts are dependent on the steric and electronic environment at the silicon centre.

Among the synthesised series, R = Me and X = Cl was found to be a good FLP adduct in reducing CO₂ to methoxyboranes (R₂BOMe) using 9-BBN as a reducing agent both in a stoichiometric and catalytic way. The authors carried out DFT calculations in support of their experimental results to explore the role of N/Si⁺ FLP-CO₂ adducts in the catalytic reduction of CO₂ with different boranes.¹³⁰ They synthesised a series of *o*-phenylene-bridged phosphorus–silicon Lewis pairs and investigated their reactivity towards CO₂ but no reaction was observed.¹³¹ Stephan and co-workers applied silyl triflates of the form R_{4–n}Si(OTf)_n (R = C₆F₅, Ph, Me; n = 1, 2; OTf = OSO₂CF₃) to activate CO₂ for





Scheme 55 Si-based CO₂ adducts using silyl triflates as Lewis acids.

adduct formation with bulky amines and phosphines (Scheme 55). Silyl triflates Ph₂SiOTf₂ and R₃SiOTf (R = C₆F₅, Ph, Me) with TMP formed the silyl carbamates **92**. Trialkylphosphines also activate CO₂ in combination with the silyl triflate generating FLP-CO₂ adducts **93**, with the silyl triflates R₃SiOTf showing reversible CO₂ binding. The bis-CO₂ adduct **94** was obtained at lower temperature (−40 °C) and using excess phosphine.¹³²

Germanium and tin FLPs for CO₂ activation

It has been proven that the cleavage of FLP-CO₂ adducts are quite difficult to great extent due to the strong hard-hard interaction of oxygen and the typical hard Lewis acids used in the FLP system according to the HSAB principle.¹³³ Ge and Sn are softer elements and are less oxophilic, thus their use could provide beneficial to enable catalytic CO₂ reduction. Although FLPs with a germanium Lewis acidic centre are known and have been shown to activate small molecules, their use in CO₂ activation and conversion is not yet reported.¹³⁴

Mitzel and co-workers reported in 2019 the synthesis of a geminal Sn/P FLP (F₅C₂)₃SnCH₂PtBu₂ by reacting LiCH₂PtBu₂ with (F₅C₂)₃SnCl. When the FLP (F₅C₂)₃SnCH₂PtBu₂ was exposed to CO₂ at −70 °C, it formed an adduct that was found to be reversible at 25 °C.¹³⁵ Fernandez performed a theoretical analysis of the FLP systems (F₅C₂)₃E-CH₂-PtBu₂ (E = Si, Ge, Sn) to understand the effect of the nature of these group 14 elements on their reactivity. Moving down the group, the reactivity of these species is kinetically enhanced (Si < Ge < Sn). Quantitatively, this trend of reactivity was analysed by the “activation strain model” of reactivity in combination with the energy decomposition analysis method. A five-membered TS with CO₂ lead to the experimentally observed zwitterionic products. The model identifies the interaction energy between the deformed reactants as the main factor controlling the reactivity of these geminal FLPs containing Si/Ge/Sn, where the lone pair of phosphorus donates into the π* orbital of C=O and a stronger electrostatic and orbital interaction is observed for Sn over Si.¹³⁶ Similarly, Pati and co-workers computationally



Fig. 9 Substrates and intermediates involved in the FLP activation of CO₂.

explored the ability of the FLP system (F₅C₂)₃E-CH₂-D(*t*Bu)₂ where E = Si, Ge, Sn and D = P, N to act as hydrogenation catalysts using CO₂ as a substrate.¹³⁷ For the FLPs where D = N, simultaneous proton and hydride migration take place, whereas for D = P FLPs, proton transfer is followed by hydride transfer. NBO analysis shows that LP(O) → σ*(D-H) and σ(E-H) → π*(C=O) dominate along the energy profile. From their studies, they predict that FLP (C₂F₅)₃Sn-CH₂-N(*t*Bu)₂ would be able to perform CO₂ hydrogenation particularly well.

Hulla reported an application of tin-based FLPs in the form R₃SnX/N-base (R = alkyl and X = OTf[−] or NTf₂[−]) which can catalyse the formation of azoles from *ortho*-substituted anilines *via* complete deoxygenation of CO₂ in the presence of H₂.¹³⁸

Computational insights into group 13 and 14 Lewis acids in FLP catalysed CO₂ activation

Grimme reported mechanistic insights, based on extensive DFT calculations, on all steps of the FLP catalysed reduction of CO₂ to boryl formate, H₂CO, bis(boryl) acetal, and methoxyl borane products in 2020.¹³⁹ The work addressed three FLP catalysts that had been previously reported; (i) Fontaine’s B/P intramolecular FLP reported in 2013,^{55,56} (ii) Stephan’s intermolecular FLP consisting of *t*Bu₃P and 9-BBN from 2014,⁵⁸ and (iii) Cantat’s 2016 Si/N FLP with 9-BBN (Fig. 9, top).¹³⁰ The report unveils the importance of the Lewis-basic CH₂O “oxide” site in promoting a hydride transfer, from calculations (PW6B95-D3+COSMO-RS//TPSS-D3+COSMO level of theory in THF). Initial formation of a zwitterionic FLP-H₂CO adduct had been proposed previously and was verified in this report, in the intramolecular FLP reported by Fontaine, this is generated through the Lewis-basic Bcat oxygen atoms **95** (Fig. 9).

Subsequent hydride transfer from the FLP-H₂CO adduct to CO₂ then forms boryl formate HCOOBcat through a series of steps, identifying the Lewis acidic Bcat group as the ‘base shuttle’. For Stephan’s intermolecular *t*Bu₃P/9-BBN FLP, a hydride transfer from *t*Bu₃P-CH₂O-9-BBN to CO₂ *via* **96** (Fig. 9) is exergonic by −16.1 kcal mol^{−1} with a barrier of 7.2 kcal mol^{−1}, which is feasible at room temperature. The final reduction step from H₂C(O-9-BBN)₂ into H₃CO-9-BBN is the slowest reduction step, with a barrier of 23.3 kcal mol^{−1}. Lastly, when investigating the mechanism for Cantat’s Si/N FLP,



Grimme and co-workers found the neutral adduct between the Lewis-basic N and 9-BBN to be the most energetically favourable starting point. Here, the B-H is partially activated by the Si/N centres. Hydride transfer to CO₂ is then exergonic by $-7.5 \text{ kcal mol}^{-1}$ via **97** (Fig. 9). In summary, zwitterionic FLP-H₂CO adducts were found to be the active catalysts, strong oxygen and nitrogen Lewis bases were found to stabilise the hydride transfer steps to CO₂, and finally, Lewis-acidic groups such as Beat were found to act as a base shuttle.

Group 15 Lewis acids

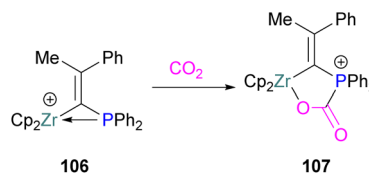
Generally, in FLP chemistry, group 15 elements are employed as the Lewis base component due to the presence of a lone pair when in the +3 oxidation state. Although nitrogen Lewis acids are known in FLPs, and have been used for small molecule activation, their application for CO₂ activation has not been explored.¹⁴⁰ On the other hand, there are a few examples using phosphorus as the Lewis acid. An example was reported by Stephan who prepared a CO₂-adduct **98** based on intramolecular amidophosphoranes where the phosphorus acts as a Lewis acidic centre and a nitrogen centre in the parent FLP acts as a nucleophilic centre to capture CO₂ (1 atm) at ambient temperatures. Similarly, the bis-CO₂-adduct **99** (Fig. 10) was also prepared under the same reaction conditions.¹⁴¹ A detailed computational mechanism was studied for the adduct **98** by Zhu and co-workers. They investigated that ring strain, and the *trans*-influence are the key factors in amidophosphoranes to capture CO₂.¹⁴²

Transition metal Lewis acids

Earlier we have discussed examples of how low valent transition metals can act as the Lewis base of an FLP when combined with boron Lewis acids. In this section we will discuss selected reports where the transition metal behaves as the Lewis acid to activate CO₂ in an FLP fashion. Several early examples by Piers reported the use of Lewis acidic scandium complexes in combination with B(C₆F₅)₃ and a silane to be operative under an FLP type mechanism to reduce CO₂.^{143,144} Examples by Wass and co-workers in 2011, however, were the first to extend the concept of FLPs to transition metals through the use of cationic zirconocene-phosphinoaryloxide complexes.¹⁴⁵ Wass reported the synthesis of zirconocene-phosphinoaryloxide complexes **100** and their applications in the FLP activation of H₂ to generate **101** and activation of CO₂ to give the FLP-CO₂ adduct **102**. **102** showed no further reaction with H₂, however **101** could insert



Scheme 56 Reaction of zirconium FLPs with H₂ and with CO₂. X[−] = [B(C₆F₅)₃][−], Cp = cyclopentadienyl, C₆H₅; Cp* = pentamethylcyclopentadienyl, C₅Me₅.



Scheme 57 Zr⁺/P Pair system in activation of CO₂.

into CO₂ under mild conditions to generate **103** (Scheme 56, top). A similar system also reported by Wass focuses on intermolecular zirconium/phosphorus FLPs where a zirconium(IV) cation **104** is combined with a tertiary phosphine. Activation of CO₂ occurred under mild conditions to yield the adduct **105** (Scheme 56, bottom).¹⁴⁶

Systematic modification of the phosphine Lewis base showed that FLPs with modest Tolman steric parameters are highly reactive and have the maximum selectivity for the intended product. The base was found to affect the selectivity, and PET₃ gave the cleanest results. These later findings demonstrate that transition metal FLPs do not require intramolecular systems and allow for the construction of intermolecular transition metal frustrated or cooperative Lewis pairs. Another zirconium based FLP has been reported by Erker in the form of an intramolecular cationic geminal Zr⁺/P pair **106** which could react with CO₂ to form a five-membered metal-laheterocyclic adduct **107** (Scheme 57).¹⁴⁷ Systems based on **106** have been the subject of theoretical studies for the reactivity of the Zr⁺/P pair system in the activation of CO₂.¹⁴⁸ Whereas, computational investigations reveal that the activation reaction

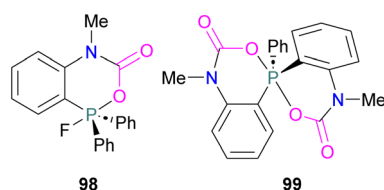
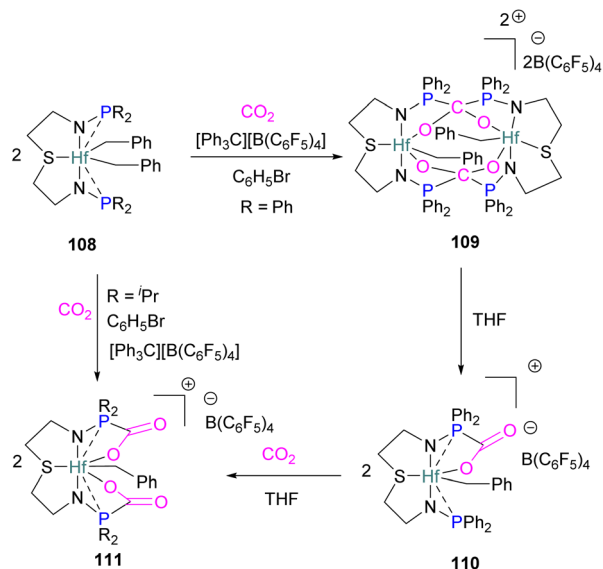


Fig. 10 Phosphorus as a Lewis acid in CO₂ capture.



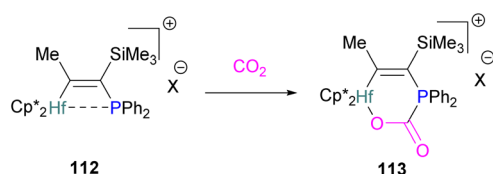


Scheme 58 CO₂ adduct formation using an intramolecular hafnium FLP.

between CO₂ and Zr⁺/P-based FLP-associated compounds is exothermic and coherent, generating a cyclic ring. The Zr⁺-P bond length contributes to the reactivity of these compounds. The donor-acceptor relationship was also found to determine the bonding nature of the activation reactions between CO₂ and Zr⁺/P-based FLP-related compounds. Accordingly, the calculated O=C=O bond stretching distance and O=C=O bending angle relate to the activation energy for CO₂ activation reactions with Zr⁺/P-based FLP-related compounds, in line with Hammond's postulate.

The heavier group 4 metal hafnium has also been shown to undergo FLP-type CO₂ activation between the metal centre and a pendant Lewis basic centre on the ligand.

The hafnium complex **108** was found to react with one or two equivalents of CO₂ to give a series of monometallic and bimetallic CO₂ activated products (**109–111**) depending upon the substituents on the phosphine ligand (Scheme 58).¹⁴⁹ In



Scheme 59 Vicinal hafnium FLP for CO₂ activation. X⁻ = [B(C₆F₅)₄]⁻.



Scheme 60 Tungsten-accelerated CO₂ activation.

these complexes, the phosphinoamines binds to hafnium *via* the nitrogen atom, and binds weakly through the softer phosphorus atom. Reaction of metallocene cation complexes [Cp*₂HfMe][B(C₆F₅)₄] with trimethylsilyl-(diarylphosphino) acetylenes yielded internal phosphane stabilised hafnium cations [Cp*₂Hf-C(Me)-C(SiMe₃)PPh₂][B(C₆F₅)₄]. As with other vicinal compounds, Hf⁺/P **112** exhibits FLP-like reactivity and generates the adduct **113** when reacted with CO₂ (Scheme 59).¹⁵⁰

An alternative approach is to use a transition metal to assist CO₂ activation as demonstrated by Streubel and co-workers. The 3-imino-azaphosphiridine complex **114** was prepared and reacted with CO₂ to obtain a heterocyclic compound **115** (Scheme 60).¹⁵¹

While numerous creative strategies are being developed for CO₂ capture, there is an increasing interest in using carbon dioxide as a C1 carbon source. The hydrogenation of CO₂ to formic acid and its derivatives is one such well-developed strategy based on Ru.¹⁵² In 2012, Stephan and co-workers developed an elegant catalytic system based on ruthenium hydride **116** (Scheme 61). This salt was explored in the reduction of CO₂ catalytically using HBpin as a reducing agent. One equivalent of **116** and 18 equivalents of HBpin under an atmosphere of CO₂ gave the MeOBPin product catalytically after 96 h at 50 °C. Increasing the ratio of **116**:HBpin to 1:100 resulted in a small increase in the TON.¹⁵³ In this system the RuNP ring in the catalyst is similar to FLP systems, and the binding of CO₂ depends upon the cooperative action of the Lewis acidic metal centre with one of the Lewis basic phosphine centres in the ligand. Cleavage of the C-P bond upon reduction with HBpin and a transfer of oxygen from Ru to Bpin allows the system for a catalytic hydroboration of CO₂. A similar cooperativity between metal and ligand was observed by Crispin and co-workers¹⁵⁴ who reported the synthesis of iridium-pyridylidene complexes [Tp^{Me2}Ir(C₆H₅)₂C(CH₃)₃C(R)NH] (Tp^{Me2} = hydrotris(3,5-dimethylpyrazolyl)borate; R = H, Me, Ph) **117**.

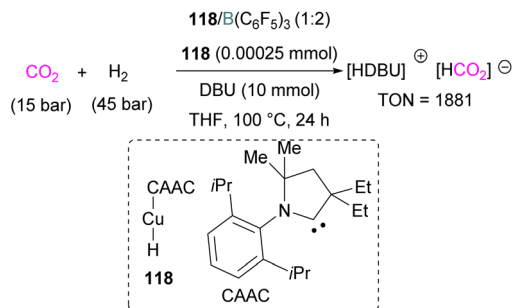


Scheme 61 Catalytic reduction of CO₂ using a Ru-H salt and pinBH.



Scheme 62 Cooperative activation of CO₂ using an iridium catalyst.



Scheme 63 Catalytic reduction of CO₂ with Cu–H/Lewis pair system.

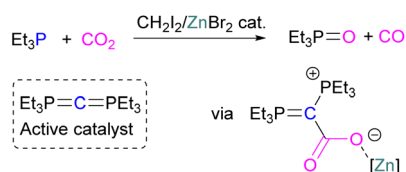
These species can activate a range of small molecules including CO₂ (R=H) in an FLP fashion between a Lewis acidic iridium centre and a Lewis basic nitrogen atom on the pyridyl ligand (Scheme 62).

Similar to the tungsten system described earlier, other metals have been employed to assist classical FLPs in CO₂ reduction. A copper-hydride system has been developed by Bertrand and co-workers for the activation and reduction of CO₂ in synergy with a N/B FLP. Amongst several screened reactions, both stoichiometric as well as catalytic, the authors found that a catalytic system consisting of a (CAAC)CuH (CAAC = cyclic (alkyl)(amino)carbene) **118** with B(C₆F₅)₃ in a 1 : 2 ratio and DBU (10 mmol) forms the formate salts of DBU from CO₂ (15 bar) and H₂ (45 bar) when heating the reaction mixture at 100 °C for 24 h in THF (Scheme 63). The key step in this reaction is the insertion of CO₂ into the copper hydride and regeneration of copper hydride with H₂. While the Cu–H bond readily inserts CO₂, it is difficult for copper to activate H₂. Thus, the FLP assists by activating H₂ to allow regeneration of the copper hydride. The TON for this reaction is observed as 1881.¹⁵⁵

Zinc metal has been explored for the reduction of CO₂ to CO. Stephan reported the *in situ* formation of the catalytically active species Et₃P=C=PEt₃ through the reduction of CO₂ to CO employing CH₂I₂.

This (bis)ylide was found to interact with CO₂, eliminating the phosphine oxide Et₃PO as a by-product and forming an interim phosphaketene. The addition of catalytic ZnBr₂ was found to facilitate the process through an FLP-type activation mode and was important for the regeneration of the (bis)ylide with simultaneous removal of CO (Scheme 64).¹⁵⁶ The same authors described Zn-based FLP chemistry for functionalising CO₂, using *t*Bu₃P/ZnEt₂ FLPs.¹⁵⁷

The transition metal based Lewis acids in the activation of CO₂ benefit from a higher coordination number when compared to the lighter main-group Lewis acids that were

Scheme 64 Reduction of CO₂ using phosphaketene/Zn FLPs.

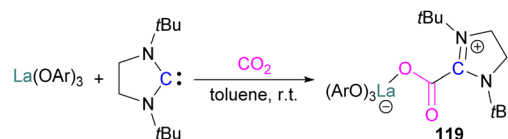
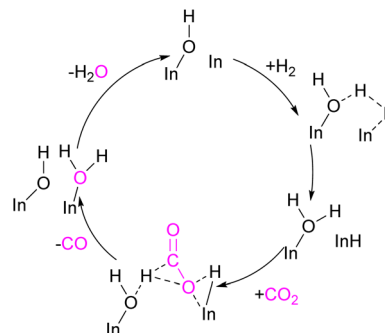
discussed previously. The ability of the TM species, such as in **110** and **116**, to bind CO₂ as well as ligand systems in more intricate intermediary species offers a higher degree of fine-tuning of the stability of adducts formed. Hence, higher turnover numbers may be observed for transition metal systems, as regeneration of the active catalyst species is kinetically more favourable. This may also explain for the more accessible use of H₂ as the reducing source compared to silanes or hydrogen surrogates often used for the main group systems. This is seen for **118** and **100**, whereas main group based Lewis acids frequently require pre-organised reducing sources, limiting the reaction to hydroboration or hydrosilylation of CO₂ rather than direct hydrogenation. Nonetheless, concerns of toxicity and environmental impact drive an increased interest in transition metal free reagents. The work on main-group CO₂ activation has focused on mimicking transition metals in synergistically accepting and donating electrons in the activation of CO₂ with species that combine filled and vacant orbitals.

Rare earth metals

Rare earth metals are often employed as Lewis acids for a variety of reactions, and have also been employed as Lewis acids in FLPs. Dihydrogen was readily activated by combination of homoleptic rare-earth metal aryloxides, RE(OAr)₃ (RE = La, Sm, and Y) with *N*-heterocyclic carbenes (NHCs) under mild conditions. In addition, the La/NHC pair exhibited FLP-like reactivity towards carbon dioxide, affording 1,2-addition products **119**, as shown in Scheme 65.¹⁵⁸

Heterogenous FLPs

Recent discoveries of FLPs as homogeneous catalysts has more recently turned to heterogeneous catalysts which operate by an FLP-type mechanism in which the Lewis acidic and Lewis basic

Scheme 65 La-in CO₂ activation. Ar = 2,6-*t*Bu₂C₆H₃.Scheme 66 In-FLP mediated CO₂ reduction.

centres in the solid structure activate CO_2 . Here, the understanding the chemistry of reactants, intermediates, and products on surfaces is crucial for designing catalytic nanostructures that transform carbon dioxide into carbon-based fuels. Several systems have been reported using indium as a Lewis acid. For example, indium oxide nanocrystals, $\text{In}_2\text{O}_{3x}(\text{OH})_y$, can catalyse the reverse water gas shift reaction, reducing carbon dioxide to carbon monoxide and water.¹⁵⁹ Surface hydroxide groups and oxygen vacancies facilitate this reaction as shown in Scheme 66.

The enhancement of activity in the gas-phase reverse water gas shift process has also been investigated, as well as the distinct photoactive behaviour of pristine and defective indium oxide surfaces.¹⁶⁰ Based on TD-DFT calculations, this study discovered that surface FLP in $\text{In}_2\text{O}_{3x}(\text{OH})_y$ has Lewis acidic indium sites close to a Lewis basic surface hydroxide. These acquired more acidity/basicity making them more active in the excited state relative to the ground state. In the photochemical reaction this reduces the activation energy relative to the thermal reaction, and could provide a mechanism to design improved photocatalytic systems for solar fuel production. In 2018, Ozin and co-workers, reported a similar system based on a rod-like nanocrystal superstructure of $\text{In}_2\text{O}_{3-x}(\text{OH})_y$, that could effectively catalyse the hydrogenation of CO_2 to methanol under light at atmospheric pressure. The rate of conversion was found to be $0.06 \text{ mmol g}^{-1} \text{ h}^{-1}$ with a 50% selectivity and a long-term working stability.¹⁶¹

Another heterogenous system based on indium has been developed by Wang and co-workers (Fig. 11). The authors developed a photocatalytic material based on a $\text{ZnIn}_2\text{S}_4/\text{In}(\text{OH})_{3-x}$ heterojunction that works in a cooperative fashion to reduce CO_2 into CO driven by light. The ZnIn_2S_4 functions to harvest the light and transport an electron to the FLP-activated CO_2 on the $\text{In}(\text{OH})_{3-x}$ surface. In $\text{In}(\text{OH})_{3-x}$, the hydroxyl-deficient vacancies (OH_{vs}) acts as a Lewis acid, and the adjacent hydroxyl groups act as a Lewis base generating the FLP which activates CO_2 . This composite showed a CO formation rate of $1945.5 \text{ } \mu\text{mol g}^{-1} \text{ h}^{-1}$.¹⁶²

Above we have seen that heterogenous FLPs can capture and react with H_2 and CO_2 , boosting photocatalytic CO_2 reduction. Isomorphous substitution of In^{3+} with Bi^{3+} has been found to increase catalytically active surface FLPs. Isomorphous substitution optimises surface catalytic active sites and affects optoelectronic characteristics, improving our understanding of photocatalytic CO_2 reduction. Such isomorphous substitution will help to develop CO_2 reduction materials with higher

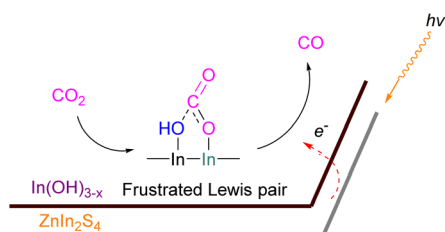
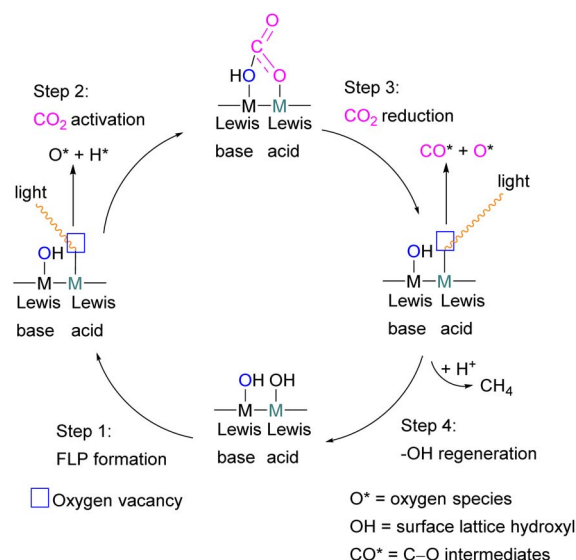


Fig. 11 An FLP $\text{ZnIn}_2\text{S}_4/\text{In}(\text{OH})_{3-x}$ (ZIOS) heterojunction system for the reduction of CO_2 to CO .

catalytic performance by tuning surface FLP site strength.¹⁶³ Another bismuth containing heterogenous system has been reported by Wang who synthesised Sn-doped BiOBr with oxygen vacancies. The synthesised material possesses surface frustrated Lewis acidic (bismuth) and Lewis basic (lattice oxygen) pairs in BiOBr through the substitution of Bi^{3+} with Sn^{4+} . 4Sn-BiOBr showed the best performance for photocatalytic CO_2 reduction into CO with a yield of $165.6 \text{ } \mu\text{mol g}^{-1} \text{ h}^{-1}$.¹⁶⁴ Another main group heterogenous system also reported is B_3P_3 doped hexa-cata-hexabenzocoronene, a model of nanographene ($\text{B}_3\text{P}_3 \cdot \text{NG}$) which reacted with carbon dioxide. This multi FLP device binds three CO_2 molecules sequentially or simultaneously on the $\text{B}_3\text{P}_3 \cdot \text{NG}$ surface.¹⁶⁵ For the CO_2 reduction *via* dissociative chemisorption of H_2 , nanocarbon-based FLP bifunctional catalysts are becoming promising due to their unquenched electron transport capability. One study proposes a nanocarbon-based FLP catalyst for the CO_2 reduction *via* the dissociative chemisorption of H_2 .¹⁶⁶

The catalyst consists of nitrogen/phosphorus doped graphene and $\text{M}(\text{C}_6\text{F}_5)_3$ ($\text{M} = \text{B}, \text{Al}, \text{Ga}, \text{In}$) as Lewis acids. The study demonstrates the potential of doped carbon-based FLPs as innovative nanostructure catalysts for CO_2 reduction *via* molecular hydrogen. N-doped FLP catalysts with activation barriers between 0.01 and 0.11 eV are promising for CO_2 reduction, potentially enabling CO_2 reduction catalytic material design.

Converting and storing solar energy through light-driven CO_2 reduction is a promising area of research. A particular approach for converting CO_2 to methane gas uses hydroxyls inherent on an oxyhydroxide photocatalyst, such as in $\text{CoGeO}_2(\text{OH})_2$, as a proton source. Irradiation of $\text{CoGeO}_2(\text{OH})_2$ causes the lattice hydroxyls to be oxidised by photogenerated holes, leading to the formation of oxygen vacancies (OVs) and protons. These OVs and Lewis acid-base pairs bind CO_2 and protons to activate it before reducing it to CH_4 . In the presence



Scheme 67 Heterogenous Ge FLP in the reduction of CO_2 to CH_4 . $\text{M} = \text{Metallic element}$.

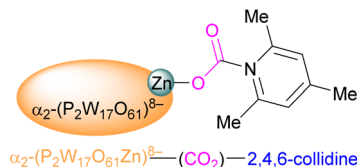


Fig. 12 CO₂ coordinated with $\alpha_2\text{-(P}_2\text{W}_{17}\text{O}_{61}\text{Zn)}^{8-}$ and 2,4,6-collidine.



Fig. 13 Photocatalytic reduction of CO₂ with FLP-TiO_{2-x}.

of water molecules, the surface lattice hydroxyls regenerate, allowing for continuous CO₂ conversion as shown in Scheme 67. This strategy has the potential to pave the way for a novel use of photocatalysis in the field of energy conversion.¹⁶⁷

Zinc based heterogeneous systems have also been reported. Neumann and co-workers studied the coordination of CO₂ to a Zn(II) Lewis acid site in Wells–Dawson type polyoxometalates $\alpha_2\text{-(P}_2\text{W}_{17}\text{O}_{61}\text{Zn)}^{8-}$ which bound CO₂ in an FLP fashion (Fig. 12). This system reveals two distinct binding modes: stronger “side-on” binding at higher temperatures and weaker “end-on” architectures at lower temperatures.¹⁶⁸ This interaction with 2,4,6-collidine is possible through the development of a frustrated Lewis pair at lower temperatures.

Like the indium oxide systems described above, efficient photocatalysts for CO₂ reduction have also been reported using titanium. Anatase TiO_{2-x} hierarchical hollow boxes with FLPs can be synthesised through *in situ* topological modification of perovskite as shown in Fig. 13. These structures possess strong adsorption and activation properties, converting CO₂ to CO without auxiliary substances. This innovative approach converts solar energy into chemical energy.¹⁶⁹

The above examples of heterogeneous FLPs are important for the activation of CO₂ compared to synthesising FLP-CO₂ adducts.

There are some challenges to select suitable methods for achieving light absorption, electron–hole separation, energy gap matching for the reduction of CO₂ to different products (product selectivity) in a photochemical way. The examples In₂O_{3x}(OH)_y, ZnIn₂S₄/In(OH)_{3-x}, 4Sn–BiOBr, and CoGeO₂(OH)₂ are promising systems for the photochemical reduction of CO₂. The use of clean sources of the reducing agent H₂ in these systems will suppress the chemical waste which is generated when activated reducing agents for the reduction of CO₂ adducts are used.

Several reports of cerium as a Lewis acid in heterogeneous FLPs are reported. Qu synthesised a defect-enriched cerium oxides (CeO₂) with constructed interfacial FLPs (Ce³⁺...O²⁻) that activate CO₂ efficiently *via* the interactions between the carbon atom of the CO₂ molecule with the Lewis basic lattice O²⁻ in CeO₂, and the two oxygen atoms of CO₂ with two adjacent



Scheme 68 CO₂ reduction using a CeO₂ surface FLP to monomethylcarbonate.

Lewis acidic Ce³⁺ centres in CeO₂. This CeO₂ solid material showed FLP-inspired tandem activation of CO₂ and reactions with alkenes to catalytically form selective cyclic carbonates.¹⁷⁰ Davide *et al.* reported that CO₂ activation is shown to occur *via* a bidentate carbonate bridging the FLP through a Ce³⁺-to-CO₂ charge transfer (Scheme 68).¹⁷¹ The authors performed a detailed study of the system in which an FLP was formed over a highly defective sample of CeO₂.

The reaction of CO₂ with MeOH formed monomethylcarbonate through an FLP mechanism involving Ce³⁺ and oxygen vacancies.

Recently, other cerium based FLP systems have also been explored for the reduction of CO₂ into products such as CH₄ and carbonates.¹⁷²

Finally, it should be noted that there are several metal organic framework (MOF) systems that have Lewis acidic metal centres and Lewis basic ligands that can also act in an FLP manner to activate CO₂.^{173–175}

Stoichiometric and catalytic reduction of CO₂: scope and limitations

So far, we have witnessed a wealth of FLP systems for CO₂ activation and reduction to different products. In this final section we summarise the key findings of the different FLP systems described in terms of CO₂ activation and the stability of the CO₂ adducts, as well as the CO₂ reduction strategies using hydrogen, silane or borane reducing agents.

An insight into the stability of CO₂ adducts

In this review many different FLP adducts with CO₂ are discussed. Stability of the FLP-CO₂ adducts is dependent on different factors, such as the state of the system (solid or solution phase), temperature and conditions (*e.g.* such as applying vacuum), the strength of the Lewis base-C (CO₂) and Lewis acid-O (CO₂) bonds, steric effects around the ligand attached to the acidic or basic reactive centre, and the geometry of the FLP system either as intra- or intermolecular systems. Several systems undergo reversible CO₂ activation which is highly



dependent upon the geometry of the FLP (intra- or intermolecular) as well as the electronic and steric effects at the Lewis acid and basic sites. Among the described examples of the FLP systems for CO₂ activation, the first was described for the B/P intra- and intermolecular systems. The FLP *t*Bu₃P/B(C₆F₅)₃ with CO₂ was observed to form a stable adduct *t*Bu₃P-CO₂-B(C₆F₅)₃ at room temperature but, upon heating under vacuum releases CO₂ and regenerates the FLP. The same outcome was observed for intramolecular system **2**, which produces a cyclic adduct with CO₂ with lower stability which decomposes even at -20 °C.³⁴ When the Lewis base and acid are aligned in a geminal fashion, an increase in reactivity is observed as seen in the formation of adduct **10** with a non-fluorinated FLP.⁴² A unique binding mode of CO₂ in the FLP system bis-borane was observed that resulted in compound **9** as a six-membered stable adduct in which two boron Lewis acidic centres in the FLP bind to the two oxygen atoms in the CO₂ molecule. This, however, was not the case for the FLP *t*Bu₃P/O(B(C₆F₅)₂)₂, where chelation of CO₂ by two B-centres was not observed due to steric effects and as well as a significant π-character in the B-O bonds supported by crystal structure information.⁴¹ With the more Lewis acidic and oxophilic aluminium Lewis acids, more stable CO₂ adducts were typically observed and in several cases both oxygen atoms of CO₂ bound to a Lewis acidic site, through coordination to two aluminium centres for example in compounds **74–76** and **78**.^{103,111} The binding strength could be tuned by varying the substituents on aluminium. The more Lewis acidic centres -AlCl₂ and -Al(C₆F₅)₂ bind CO₂ irreversibly, while less Lewis acidic -AlMeCl binds CO₂ reversibly under 2 bar CO₂, liberating CO₂ when the excess pressure is released. For catalytic applications, this reversible binding is necessary to enable release of the product. In several cases, not only CO₂ activation is observed but also further reactivity of the adduct with the FLP to generate more stable CO₂ activated products. These reactions, however, would be irreversible and therefore stoichiometric. Examples of this have been observed in the B/N FLP **34** in which a cyclohexyl group migrates from boron to an adjacent carbon centre.⁷² Overall, in the activation of CO₂ molecule specially in the homogeneous FLP-CO₂ adduct systems, a species that can reversibly form weak adducts of CO₂ with almost no energy barrier in either direction would be an incredible valuable tool to enable catalytic transformations. Alternatively, combinations of LA and LB are promising that show reversible CO₂ binding. Homogeneous and heterogeneous metal based FLP systems have been shown to be very promising in the activation of CO₂ through an FLP mechanism and offer much promise for catalytic turnover (see later).

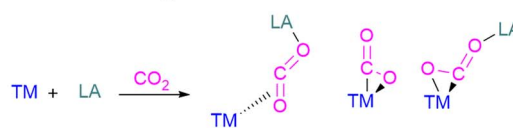
CO₂ reductions in FLP systems

As we have seen in this review, the binding and activation modes of small molecules (in this case CO₂ and H₂) are different in homogeneous (metals and non-metal in inter- and intramolecular) and heterogeneous FLP systems. In homogeneous systems, the combination of Lewis base and acid in frustrated pairs typically cleave the H-H bond heterolytically and form ion pairs [LB-H]⁺[LA-H]⁻. [LA-H]⁻ acts as a hydride source and can

A. Activation of CO₂ by LA-H



B. Activation of CO₂ with transition metal/Lewis acid FLPs



C. Activation of CO₂ with transition metal/Lewis base FLPs



D. Activation of CO₂ in heterogeneous FLPs

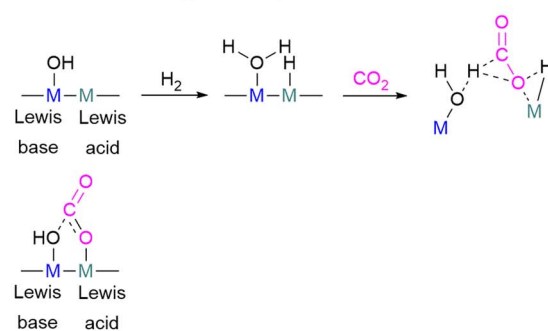


Fig. 14 CO₂ activation mode in different FLP systems.

reduce CO₂ by transferring H⁻ to the carbon atom. The oxygen anion generated is then trapped by the Lewis acid generating formates (Fig. 14A). The formation of formate salts of CO₂ with H₂ surrogates [LB-H]⁺[LA-H]⁻ are shown as examples in Schemes 12, 24 and 25. To utilise this strategy for CO₂ reduction in a catalytic way has been studied computationally showing a possible reduction of CO₂ to HCO₂H in Schemes 15 and 16 but practically has not been demonstrated. For a practical feasibility, the ion pair [LB-H]⁺ should be able to supply H⁺ to the formed formate ion [HCOO-LA]⁻. If this occurs, then the FLP would catalyse hydrogenation of CO₂, but the limiting factor is the release of the formate from [HCOO-LA]⁻ due to the strength of the O-LA bond. In other words, for a catalytic hydrogenation of CO₂ using FLPs, the ion pair [LB-H]⁺[LA-H]⁻ should regenerate the free Lewis acid and base following CO₂ reduction. This remains a key challenge in main group FLP-CO₂ reduction and the use of a strong Lewis acid often precludes product release. One strategy to overcome this could be to use inverse frustrated Lewis pair systems. This was observed for the use of excess Lewis base DBU in combination with the Lewis acid tbtb (tris(*p*-bromo)tridurylborane), an inverse FLP as shown in Scheme 31.⁸³ Another example of catalytic hydrogenation of CO₂ to formate was explored by using K₂CO₃/B(C₆F₅)₃ with H₂.¹⁰²

Metal systems as a Lewis basic centre in combination with a Lewis acid show a different way of activating CO₂ and coordinate to the CO₂ molecule through the C=O bond (Fig. 14B) as



seen with Lewis basic Pt, Re and Mo systems. The Lewis acidic component of the FLP then activates the oxygen atom. CO₂ can be found in a reduced state with a Re system where reduction to formate is observed through CO₂ hydrogenation using H₂. When the transition metal is incorporated as the Lewis acid component of an FLP, then the mode of CO₂ activation is similar to that observed for the main group Lewis acids with TM–O bond formation (Fig. 14C). Here, it is interesting to note that the system before reaction with CO₂ can cleave H₂ heterolytically, similar to other FLPs and the TM–H bond then inserts into the CO₂ molecule. An example for this type of reaction is shown for cationic zirconocene–phosphinoaryloxy complexes in Scheme 56.

Heterogeneous FLPs systems activate CO₂ using a similar concept but *via* a different mechanism (Fig. 14D) and are generally not limited by some of the challenges that main group systems face. In these systems the surface has Lewis acidic metal sites such as indium or titanium. However, the Lewis basic sites are typically an oxygen atom (often as a hydroxy group). This tolerance to hydroxy functional groups is a significant advantage in the heterogeneous systems and provides easier routes for CO₂ reduction. In many of the main group FLP systems described herein the strong binding to oxygen centres, while beneficial for CO₂ activation, is detrimental to catalytic turnover.

CO₂ reduction by FLPs: using H₂, activated B–H and Si–H

Several catalytic reduction methods have been developed utilising different FLP systems using different reducing agents. For CO₂ reduction, direct hydrogenation provides the best approach as it is clean and generates no waste. However, many FLP systems, especially those using the main group elements, have used other reducing agents such as silanes or boranes due to the inability of the system to activate H₂ in conjunction with CO₂. Thus, although some FLPs showed promising results for the CO₂ reduction with a direct use of H₂ gas as a reducing agent, heterogeneous systems have shown to be more promising with the direct use of H₂. As described by several computational studies considering hydrogenation of CO₂ with only H₂ as the reducing agent, the energy barrier to the

activation of H₂ by the FLP system is generally higher than the activation barrier for that of CO₂. Fine-tuning of both the Lewis acid's ability to accept a hydride from H₂ and the Lewis base's ability to accept a proton from H₂ is necessary to consequently reduce activated CO₂. The computational work herein have highlighted the importance for a cumulative high Lewis basicity and acidity, whilst avoiding the combination of a very strong Lewis acid with a very strong Lewis base as this negatively impacts both the activation barriers to H₂ and CO₂.

For many systems seen in this review, boron reducing agents have commonly been employed in homogeneous systems, for example R₂BH/HBpin. Here either the Lewis base or acid activates the reducing agent towards reduction, as shown in Fig. 15. The first mode of CO₂ reduction with R₂BH and the Lewis base is the nucleophilic activation of R₂BH. Strong nucleophiles favor hydride transfer to CO₂ by increasing the hydridicity of the B–H bond (Fig. 15A). Alternatively, the Lewis acids may abstract the hydride of the B–H bond to yield a boron electrophile and convert the Lewis acid catalyst to a strong hydride donor (Fig. 15B).¹⁷⁶ In these two mechanisms, the Lewis acid component is then trapped by the generated oxygen anion. In these cases, the formation of stable CO₂ adducts often hampers catalysis by stabilising the catalyst's resting state. As we have seen above, the FLP catalyst can also activate the CO₂ molecule directly. As CO₂ is a weak Lewis base, this mode of action usually involves a bifunctional activation of CO₂ with the cooperative effect of a Lewis base and a Lewis acid (Fig. 15C). The borohydride reducing agent then can directly hydrogenate this species. In many cases, “activation” of CO₂ in the form of an adduct is both deleterious and necessary to the catalytic activity, as it stabilises the lowest intermediate in the potential energy surface yet prepares CO₂ for the subsequent reduction steps by removing electron density from the carbon by coordination to the Lewis acid. It is noteworthy that future catalytic systems based on this approach should be target compounds that show a lower affinity for CO₂, based on thermodynamics, yet increase the electrophilicity of the carbon centre. Instead of borane reducing agents, silanes such as Et₃SiH have also been used for catalytic CO₂ reduction. For example, using R₃SiH with a Lewis acid, an electrophilic activation is observed similar to the way shown Fig. 15B. Although several examples use H₂ as the reducing agent, this remains a challenge with main group systems and more success has been observed in this regard when using either homogenous or heterogeneous transition metal systems.

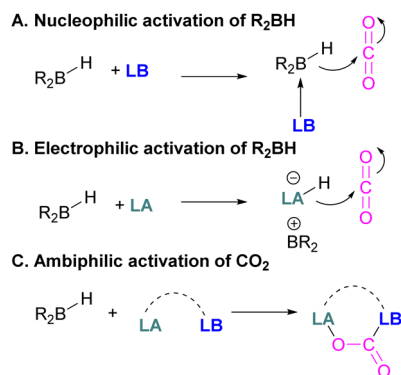


Fig. 15 Activation of boranes in CO₂ reduction.

Stoichiometric and catalytic reduction of CO₂ in FLPs

Various homogeneous and heterogeneous FLPs systems have been investigated for the reduction of CO₂. It depends on certain properties of the FLP system to guide the CO₂ reduction either for a stoichiometric or a catalytic reaction pathway. For CO₂ adducts, a strong Lewis base and a weak Lewis acid adduct of CO₂ appear suitable for catalytic CO₂ reduction whereas stronger Lewis acids form stable CO₂ adducts. To carry out a catalytic reduction of CO₂ in a zwitterionic system, a first condition is that the bond between O atom of CO₂ and the Lewis



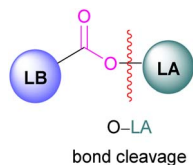


Fig. 16 Mode for facile reduction of CO₂.

acid should be weak, *i.e.* the Lewis acid should not be too acidic or oxophilic (see Fig. 16). Secondly, the cation of the activated reducing agents (R₂B-H or R₃Si-H) after supplying hydride ion should be able to trap the oxygen atom, cleaving the O-LA bond. Here, both the Lewis acid and base are not coordinated, and the system will be able to reversibly activate and reduce CO₂ leading to a catalytic pathway. Several CO₂ adduct systems have been discussed for catalytic CO₂ reductions. Intramolecular FLP **21** acts as an efficient catalyst because it does not form an adduct with CO₂ (as most of the FLPs form stable CO₂ adducts), and the CH₂O moiety is released upon reduction from the catalyst and thus makes **21** active for another turnover.^{55–57} In the *t*Bu₃P/9-BBN FLP system, hydride transfer from boron to the carbonyl carbon releases *t*Bu₃P for the next cycle, and hence this system also works catalytically.⁵⁸ Another interesting catalytic example is for the TMP/B(C₆F₅)₃ FLP system, where Et₃SiH is employed as a silane reducing agent producing Et₃Si⁺ following B(C₆F₅)₃ Si-H activation.⁷⁸ Et₃Si⁺ is a good oxygen acceptor and thus promotes the catalytic deoxygenation of CO₂ to CH₄ and (Et₃Si)₂O. Although catalytic, the stoichiometric use of silane is not desirable in the longer term and routes that employ H₂ as a hydrogen source should be sought. Making use of FLPs in direct catalytic hydrogenations of CO₂ remain difficult. Although hydride transfer from [LA-H] to CO₂ have been described in this review, the proton transfer from [LB-H] does not occur readily due to the formation of a strong O-LA bond (Fig. 16). Hence, most FLP systems are seen to terminate at adduct formation as O-LA, and although the H₂ activation barrier may have been overcome, full hydrogenation of CO₂ is prohibited. Some success has been achieved with inverse FLP systems (*e.g.* tris(*p*-bromo)tridurylborane (tbtb)/DBU).⁸³ To obtain a suitable FLP for the direct catalytic hydrogenation of CO₂, the intrinsic reactivity of each of the components is very important *i.e.*, free energy of proton attachment to the Lewis base and free energy of hydride attachment to the Lewis acid. For high turnover numbers and turnover frequencies, a catalyst should be stable enough and should regenerate in the catalytic cycle. In some of the examples, the highest in carbene system **58** using 9-BBN as the reducing agent, FLPs have shown a good TON and TOF for the reduction of CO₂. As shown in the latter part of this review, metals and heterogeneous FLPs are generally efficient to activate and use H₂ as a direct reducing source for CO₂. For example, indium oxide has been found to be a particularly good example of a heterogeneous FLP system where H₂ is directly utilised for the reduction of CO₂.¹⁵⁹ The potential of transition metals is that they provide reactive sites for the activation of H₂ as well as CO₂, but in several cases, they are not cost efficient.

Conclusions

Tremendous progress in CO₂ activation and reduction to value added products in both homogeneous and heterogeneous systems on bench scale has been seen. Both homogenous and heterogeneous transition metal systems, as Lewis acids and bases have been efficient for the reduction of CO₂. However, main group elements have emerged as alternatives and remarkable progress has been made here. Group 13 elements, boron and aluminium as Lewis acids have been heavily explored combined with Lewis bases such as phosphines, amines, or carbenes. In many cases, activation of CO₂ has been achieved up to full conversion under mild conditions, and in several examples reduced products can be obtained in the form of methanol, formates, acetates and CH₄ upon addition of a silane or borane, or in some cases H₂. Most commonly, the formation of a zwitterionic product is the initial key activation step in the reduction of CO₂. However, subsequent product liberation has been seen to be the most limiting step in these reactions, thus limiting the scope of catalytically viable reactions. Currently H₂ is utilised as a reducing agent on industrial scale as it is cheap and widely available, but its use in CO₂ reduction with FLPs is limited and other reducing agents such as hydrosilanes, hydroboranes or ammonia boranes are often used. However, a drawback of these reducing agents in CO₂ reduction is that they form strong Si-O and B-O bonds and form oxidised products such as siloxanes or boroxanes, making the process less atom economic. Thus, there still need to be significant development of FLP CO₂ reduction using H₂ as the reducing agent. Compared to main group FLP-CO₂ adduct systems, transition metals possessing empty orbitals that offer site selective coordination have been applied as more suitable systems to activate the non-polar covalent bond in H₂ and utilise this as a direct reducing source. Conversely, heterogeneous systems provide the opportunity of recycling and have also been seen to achieve higher TONs and TOFs. Present chemical methods of recycling siloxanes or boroxanes to the corresponding hydrosilanes or hydroboranes are energy intense. Electrochemical methods are efficient and have made material recycling possible. Therefore, electrochemical methods may be an attractive and efficient approach over chemical routes for recycling of the oxides to their corresponding hydrides. The key to obtain high TON for hydrosilylation, hydroboration, or hydrogenation relies on the stability of the catalyst, the release of the reduced products and then catalyst regeneration. Thermodynamic control is the main limitation in accessing CO₂ reduced products beyond carboxylates, whilst kinetic control is the main limitation in achieving high output catalytic cycles that regenerate the catalyst. Although some progress has been made to achieve CO₂ reduction in a catalytic manner, the challenge is still to achieve a robust and effective FLP system that can catalyse CO₂ reduction at ambient temperature and pressure utilising H₂ as a reducing agent. In addition, there must be more focus on selective reduction reactions to give valuable products that are of interest to industry. Further investigations should focus on developing highly active and selective FLP systems for the catalytic conversion to C₁ or C₂ products, and could include various methods for conversion such as thermal, photochemical, or electrochemical methods.



Author contributions

All authors contributed to the writing and revisions of the review.

Conflicts of interest

There are no conflicts to declare.

Acknowledgements

We would like to thank BP (Alejandro G. Barrado and Sheetal Handa) for funding, and for their guidance in preparing this review.

References

- (a) K. Abbass, M. Z. Qasim, H. Song, M. Murshed, H. Mahmood and I. Younis, *Environ. Sci. Pollut. Res.*, 2022, **29**, 42539; (b) P. C. Jain, *Renewable Energy*, 1993, **3**, 403; (c) P. J. Michaels, *Int. J. Environ. Stud.*, 1990, **36**, 55.
- C. Figueres, C. Le Quere, A. Mahindra, O. Bate, G. Whiteman, G. Peters and D. Guan, *Nature*, 2018, **564**, 27.
- (a) A. Bhavsar, D. Hingar, S. Ostwal, I. Thakkar, S. Jadeja and M. Shah, *Case Stud. Chem. Environ. Eng.*, 2023, **8**, 100368; (b) M. Bui, C. S. Adjiman, A. Bardow, E. J. Anthony, A. Boston, S. Brown, P. S. Fennell, S. Fuss, A. Galindo, L. A. Hackett, J. P. Hallett, H. J. Herzog, G. Jackson, J. Kemper, S. Krevor, G. C. Maitland, M. Matuszewski, I. S. Metcalfe, C. Petit, G. Puxty, J. Reimer, D. M. Reiner, E. S. Rubin, S. A. Scott, N. Shah, B. Smit, J. P. M. Trusler, P. Webley, J. Wilcox and N. M. Dowell, *Energy Environ. Sci.*, 2018, **11**, 1062; (c) E. I. Koysoumpa, C. Bergins and E. Kakaras, *J. Supercrit. Fluids*, 2018, **132**, 3; (d) A. Rafiee, K. R. Khalilpour, D. Milani and M. Panahi, *J. Environ. Chem. Eng.*, 2018, **6**, 5771.
- (a) For examples see: W. Gao, S. Liang, R. Wang, Q. Jiang, Y. Zhang, Q. Zheng, B. Xie, C. Y. Toe, X. Zhu, J. Wang, L. Huang, Y. Gao, Z. Wang, C. Jo, Q. Wang, L. Wang, Y. Liu, B. Louis, J. Scott, A.-C. Roger, R. Amal, H. Heh and S.-E. Park, *Chem. Soc. Rev.*, 2020, **49**, 8584; (b) S. Valluri, V. Claremboux and S. Kawatra, *J. Environ. Sci.*, 2022, **113**, 322; (c) Y. Y. Birdja, E. Pérez-Gallent, M. C. Figueiredo, A. J. Göttle, F. Calle-Vallejo and M. T. M. Koper, *Nat. Energy*, 2019, **4**, 732; (d) J. H. Park, J. Yang, D. Kim, H. Gim, W. Y. Choi and J. W. Lee, *Chem. Eng. J.*, 2022, **427**, 130980; (e) S. Navarro-Jaén, M. Virginie, J. Bonin, M. Robert, R. Wojcieszak and A. Y. Khodakov, *Nat. Rev. Chem.*, 2021, **5**, 564.
- (a) For examples see: H. Onyeaka and O. C. Ekwebelem, *Int. J. Environ. Sci. Technol.*, 2023, **20**, 4635; (b) M. A. Zahed, E. Movahed, A. Khodayari, S. Zanganeh and M. Badamaki, *J. Environ. Manage.*, 2021, **293**, 112830; (c) H. Arakawa, M. Aresta, J. N. Armor, M. A. Barteau, E. J. Beckman, A. T. Bell, J. E. Bercaw, C. Creutz, E. Dinjus, D. A. Dixon, K. Domen, D. L. DuBois, J. Eckert, E. Fujita, D. H. Gibson, W. A. Goddard, D. W. Goodman, J. Keller, G. J. Kubas, H. H. Kung, J. E. Lyons, L. E. Manzer, T. J. Marks, K. Morokuma, K. M. Nicholas, R. Periana, L. Que, J. Rostrup-Nielson, W. M. H. Sachtler, L. D. Schmidt, A. Sen, G. A. Somorjai, P. C. Stair, B. R. Stults and W. Tumas, *Chem. Rev.*, 2001, **101**, 953.
- (a) For recent examples see: A. Jana, S. W. Snyder, E. J. Crumlin and J. Qian, *Front. Chem.*, 2023, **11**, 1135829; (b) D. Wei, R. Sang, A. Moazezbarabadi, H. Junge and M. Beller, *JACS Au*, 2022, **2**, 1020; (c) R. Cauwenbergh, V. Goyal, R. Maiti, K. Natte and S. Das, *Chem. Soc. Rev.*, 2022, **51**, 9371; (d) R. Sen, A. Goeppert and G. K. S. Prakash, *Angew. Chem., Int. Ed.*, 2022, **61**, e202207278; (e) P. Sarkar, I. H. Chowdhury, S. Das and S. M. Islam, *Mater. Adv.*, 2022, **3**, 8063; (f) B. Shao, Y. Zhang, Z. Sun, J. Li, Z. Gao, Z. Xie, J. Hu and H. Liu, *Green Chem. Eng.*, 2022, **3**, 189; (g) Q. Zhang, C. Yang, A. Guan, M. Kan and G. Zheng, *Nanoscale*, 2022, **14**, 10268; (h) S. Shao, C. Cui, Z. Tang and G. Li, *Nano Res.*, 2022, **15**, 10110; (i) J. Wei, R. Yao, Y. Han, Q. Ge and J. Sun, *Chem. Soc. Rev.*, 2021, **50**, 10764; (j) F. N. Al-Rowaili, U. Zahid, S. Onaizi, M. Khaled, A. Jamal and E. M. Al-Mutairi, *J. CO₂ Util.*, 2021, **53**, 101715; (k) Z. Zhang, S.-Y. Pan, H. Li, J. Cai, A. G. Olabi, E. J. Anthony and V. Manovic, *Renewable Sustainable Energy Rev.*, 2020, **125**, 109799; (l) V. Kumaravel, J. Bartlett and S. C. Pillai, *ACS Energy Lett.*, 2020, **5**, 486.
- M. Aresta, A. Dibenedetto and A. Angelini, *Chem. Rev.*, 2014, **114**, 1709.
- I. Tebbiche, J. Mocellin, L. T. Huong and L.-C. Pasquier, 27 - Circular Economy and Carbon Capture, Utilization, and Storage, in *Circular Bioeconomy - Current Status and Future Outlook*, Biomass, Biofuels, Biochemicals, 2021, pp. 813–851.
- (a) E. A. Quadrelli, G. Centi, J.-L. Duplan and S. Perathoner, *ChemSusChem*, 2011, **4**, 1194; (b) J. Klankermayer, S. Wesselbaum, K. Beydoun and W. Leitner, *Angew. Chem., Int. Ed.*, 2016, **55**, 7296.
- J. Schneider, H. Jia, J. T. Muckerman and E. Fujita, *Chem. Soc. Rev.*, 2012, **41**, 2036.
- N. N. Greenwood and A. Earnshaw, *Chemistry of the Elements*, Butterworth-Heinemann, 2nd edn, 1997, vol. 305. ISBN 978-0-08-037941-8.
- U. J. Etim, C. Zhang and Z. Zhong, *Nanomaterials*, 2021, **11**, 3265.
- (a) For examples see: A. Takahashi, K. Minami, K. Noda, K. Sakurai and T. Kawamoto, *ACS Sustainable Chem. Eng.*, 2021, **9**, 16865; (b) A. Sayari, A. Heydari-Gorji and Y. Yang, *J. Am. Chem. Soc.*, 2012, **134**, 13834; (c) G. Puxty, R. Rowland, A. Allport, Q. Yang, M. Bown, R. Burns, M. Maeder and M. Attalla, *Environ. Sci. Technol.*, 2009, **43**, 6427; (d) J. T. Yeh, K. P. Resnik, K. Rygle and H. W. Pennline, *Fuel Process. Technol.*, 2005, **86**, 1533.
- S. Chakraborty, O. Blacque and H. Berke, *Dalton Trans.*, 2015, **44**, 6560.
- N. W. Kinzel, C. Werlé and W. Leitner, *Angew. Chem., Int. Ed.*, 2021, **60**, 11628.



- 16 (a) For examples see: Q.-J. Wu, J. Liang, Y.-B. Huang and R. Cao, *Acc. Chem. Res.*, 2022, **55**, 2978; (b) L. D. Ramírez-Valencia, E. Bailón-García, F. Carrasco-Marín and A. F. Pérez-Cadenas, *Catalysts*, 2021, **11**, 351; (c) R.-P. Ye, J. Ding, W. Gong, M. D. Argyle, Q. Zhong, Y. Wang, C. K. Russell, Z. Xu, A. G. Russell, Q. Li, M. Fan and Y.-G. Yao, *Nat. Commun.*, 2019, **10**, 5698.
- 17 G. C. Welch, R. R. San Juan, J. D. Masuda and D. W. Stephan, *Science*, 2006, **314**, 1124.
- 18 F.-G. Fontaine and D. W. Stephan, *Philos. Trans. R. Soc. A*, 2017, **375**, 20170004.
- 19 (a) For CO₂ activation see: F.-G. Fontaine and D. W. Stephan, *Curr. Opin. Green Sustainable Chem.*, 2017, **3**, 28; (b) P. Sreejothi and S. K. Mandal, *Chem. Sci.*, 2020, **11**, 10571; (c) S. Bontemps, *Coord. Chem. Rev.*, 2016, **308**, 117; (d) D. W. Stephan and G. Erker, *Chem. Sci.*, 2014, **5**, 2625; (e) A. E. Ashley and D. O'Hare, FLP-Mediated Activations and Reductions of CO₂ and CO, in *Frustrated Lewis Pairs II*, Topics in Current Chemistry, ed. G. Erker and D. W. Stephan, Springer, Berlin, Heidelberg, 2012, vol. 334, During proof-editing of this review this paper was published as an early view article; (f) M. Perez-Jimenez, H. Corona, F. de la Cruz-Martínez and J. Campos, *Chem.-Euro. J.*, 2023, **29**, e202301428.
- 20 G. N. Lewis, *Valence and the Structure of Atoms and Molecules*, Chemical Catalogue Company, Inc., New York, 1923.
- 21 H. C. Brown, H. I. Schlesinger and S. Z. Cardon, *J. Am. Chem. Soc.*, 1942, **64**, 325.
- 22 G. Wittig and A. Rückert, *Adv. Cycloaddit.*, 1950, **566**, 101.
- 23 W. Tochtermann, *Angew. Chem., Int. Ed.*, 1966, **5**, 351.
- 24 D. J. Parks and W. E. Piers, *J. Am. Chem. Soc.*, 1996, **118**, 9440.
- 25 S. Rendler and M. Oestreich, *Angew. Chem., Int. Ed.*, 2008, **47**, 5997.
- 26 J. S. J. McCahill, G. C. Welch and D. W. Stephan, *Angew. Chem., Int. Ed.*, 2007, **46**, 4968.
- 27 G. C. Welch and D. W. Stephan, *J. Am. Chem. Soc.*, 2007, **129**, 1880.
- 28 (a) L. J. C. van der Zee, S. Pahar, E. Richards, R. L. Melen and J. C. Sloatweg, *Chem. Rev.*, 2023, **123**, 9653; (b) A. Dasgupta, E. Richards and R. L. Melen, *Angew. Chem., Int. Ed.*, 2021, **60**, 53.
- 29 J. Zhu and K. An, *Chem.-Asian J.*, 2013, **8**, 3147.
- 30 (a) T. Özgün, K. Bergander, L. Liu, C. G. Daniliuc, S. Grimme, G. Kehr and G. Erker, *Chem.-Euro. J.*, 2016, **22**, 11958; (b) T. Özgün, K.-Y. Ye, C. G. Daniliuc, B. Wibbeling, L. Liu, S. Grimme, G. Kehr and G. Erker, *Chem.-Euro. J.*, 2016, **22**, 5988; (c) B. Schirmer and S. Grimme, Quantum Chemistry of FLPs and Their Activation of Small Molecules: Methodological Aspects in Frustrated Lewis Pairs I, *Top. Curr. Chem.*, 2013, **332**, 213.
- 31 L. Liu, B. Lukose and B. Ensing, *ACS Catal.*, 2018, **8**, 3376.
- 32 B. L. Thompson and Z. M. Heiden, *Tetrahedron*, 2019, **75**, 2099.
- 33 Y. Yan, J. Yu, Y. Du, S. Yan, M. Gu, W. Zhou and Z. Zou, *Cell Rep. Phys. Sci.*, 2023, **4**, 101406.
- 34 C. M. Mömming, E. Otten, G. Kehr, R. Fröhlich, S. Grimme, D. W. Stephan and G. Erker, *Angew. Chem., Int. Ed.*, 2009, **48**, 6643.
- 35 (a) M. Puand and T. Privalov, *Chem.-Euro. J.*, 2015, **21**, 17708; (b) M. Pu and T. Privalov, *Inorg. Chem.*, 2014, **53**, 4598.
- 36 I. Peuser, R. C. Neu, X. Zhao, M. Ulrich, B. Schirmer, J. A. Tannert, G. Kehr, R. Fröhlich, S. Grimme, G. Erker and D. W. Stephan, *Chem.-Euro. J.*, 2011, **17**, 9640.
- 37 M. Harhausen, R. Fröhlich, G. Kehr and G. Erker, *Organometallics*, 2012, **31**, 2801.
- 38 M. M. Hansmann, R. L. Melen, M. Rudolph, F. Rominger, H. Wadepohl, D. W. Stephan and A. S. K. Hashmi, *J. Am. Chem. Soc.*, 2015, **137**, 15469.
- 39 K. Takeuchia and D. W. Stephan, *Chem. Commun.*, 2012, **48**, 11304.
- 40 B. M. Barry, D. A. Dickie, L. J. Murphy, J. A. C. Clyburne and R. A. Kemp, *Inorg. Chem.*, 2013, **52**, 8312.
- 41 X. Zhao and D. W. Stephan, *Chem. Commun.*, 2011, **47**, 1833.
- 42 F. Bertini, V. Lyaskovskyy, B. J. J. Timmer, F. J. J. de Kanter, M. Lutz, A. W. Ehlers, J. C. Sloatweg and K. Lammertsma, *J. Am. Chem. Soc.*, 2012, **134**, 201.
- 43 M. Sajid, G. Kehr, T. Wiegand, H. Eckert, C. Schwickert, R. Pöttgen, A. J. P. Cardenas, T. H. Warren, R. Fröhlich, C. G. Daniliuc and G. Erker, *J. Am. Chem. Soc.*, 2013, **135**, 8882.
- 44 L.-M. Elmer, G. Kehr, C. G. Daniliuc, M. Siedow, H. Eckert, M. Tesch, A. Studer, K. Williams, T. H. Warren and G. Erker, *Chem.-Euro. J.*, 2017, **23**, 6056.
- 45 C. Chen, C. G. Daniliuc, C. Mück-Lichtenfeld, G. Kehr and G. Erker, *Chem. Commun.*, 2020, **56**, 8806.
- 46 X. Jie, Q. Sun, C. G. Daniliuc, R. Knitsch, M. R. Hansen, H. Eckert, G. Kehr and G. Erker, *Chem.-Euro. J.*, 2020, **26**, 1269.
- 47 N. Szykiewicz, Ł. Ponikiewski and R. Grubba, *Chem. Commun.*, 2019, **55**, 2928.
- 48 N. Szykiewicz, A. Ordyszewska, J. Chojnacki and R. Grubba, *RSC Adv.*, 2019, **9**, 27749.
- 49 N. Szykiewicz, A. Ordyszewska, J. Chojnacki and R. Grubba, *Inorg. Chem.*, 2021, **60**, 3794.
- 50 J. M. Kessete, T. B. Demissie, M. Chilume, A. M. Mohammed and V. Andrushchenko, *Mol. Phys.*, 2022, **120**, e2087566.
- 51 Z. Jian, G. Kehr, C. G. Daniliuc, B. Wibbeling and G. Erker, *Dalton Trans.*, 2017, **46**, 11715.
- 52 M. J. Sgro, J. Dömera and D. W. Stephan, *Chem. Commun.*, 2012, **48**, 7253.
- 53 S. C. Binding, H. Zaher, F. M. Chadwick and D. O'Hare, *Dalton Trans.*, 2012, **41**, 9061.
- 54 A. L. Travis, S. C. Binding, H. Zaher, T. A. Q. Arnold, J.-C. Buffeta and D. O'Hare, *Dalton Trans.*, 2013, **42**, 2431.
- 55 M.-A. Courtemanche, M.-A. Légaré, L. Maron and F.-G. Fontaine, *J. Am. Chem. Soc.*, 2013, **135**, 9326.
- 56 M.-A. Courtemanche, M.-A. Légaré, L. Maron and F.-G. Fontaine, *J. Am. Chem. Soc.*, 2014, **136**, 10708.



- 57 R. Declercq, G. Bouhadir, D. Bourissou, M.-A. Légaré, M.-A. Courtemanche, K. Sy. Nahi, N. Bouchard, F.-G. Fontaine and L. Maron, *ACS Catal.*, 2015, **5**, 2513.
- 58 T. Wang and D. W. Stephan, *Chem. Commun.*, 2014, **50**, 7007.
- 59 B. Jiang, Q. Zhang and L. Dang, *Org. Chem. Front.*, 2018, **5**, 1905.
- 60 M. Delarmelina, J. W. de M. Carneiro, C. R. A. Catlow and M. Bühl, *Catal. Commun.*, 2022, **162**, 106385.
- 61 T. A. R. Horton, M. Wang and M. P. Shaver, *Chem. Sci.*, 2022, **13**, 3845.
- 62 L. Chen, R. Liu, X. Hao and Q. Yan, *Angew. Chem., Int. Ed.*, 2019, **58**, 264.
- 63 L. Chen, R. Liu and Q. Yan, *Angew. Chem., Int. Ed.*, 2018, **57**, 9336.
- 64 K. Mentoor, L. Twigge, J. W. H. Niemantsverdriet, J. C. Swarts and E. Erasmus, *Inorg. Chem.*, 2021, **60**, 55.
- 65 F. Buß, P. Mehlmann, C. Mück-Lichtenfeld, K. Bergander and F. Dielmann, *J. Am. Chem. Soc.*, 2016, **138**, 1840.
- 66 T. Voss, T. Mahdi, E. Otten, R. Fröhlich, G. Kehr, D. W. Stephan and G. Erker, *Organometallics*, 2012, **31**, 2367.
- 67 E. Theuergarten, J. Schlösser, D. Schlüns, M. Freytag, C. G. Daniliuc, P. G. Jones and M. Tamm, *Dalton Trans.*, 2012, **41**, 9101.
- 68 M. A. Dureen and D. W. Stephan, *J. Am. Chem. Soc.*, 2010, **132**, 13559.
- 69 L. Yang, X. Ren, H. Wang, N. Zhang and S. Hong, *Res. Chem. Intermed.*, 2012, **38**, 113.
- 70 M. Ghara and P. K. Chattaraj, *Struct. Chem.*, 2019, **30**, 1067.
- 71 C. Jianga and D. W. Stephan, *Dalton Trans.*, 2013, **42**, 630.
- 72 B. R. Barnett, C. E. Moore, A. L. Rheingold and J. S. Figueroa, *Chem. Commun.*, 2015, **51**, 541.
- 73 V. Sumerin, F. Schulz, M. Nieger, M. Leskelä, T. Repo and B. Rieger, *Angew. Chem., Int. Ed.*, 2008, **47**, 6001.
- 74 A. E. Ashley, A. L. Thompson and D. O'Hare, *Angew. Chem., Int. Ed.*, 2009, **48**, 9839.
- 75 S. J. Geier and D. W. Stephan, *J. Am. Chem. Soc.*, 2009, **131**, 3476.
- 76 S. D. Tran, T. A. Tronic, W. Kaminsky, D. M. Heinekey and J. M. Mayer, *Inorg. Chim. Acta*, 2011, **369**, 126.
- 77 M.-A. Courtemanche, A. P. Pulis, É. Rochette, M.-A. Légaré, D. W. Stephan and F.-G. Fontaine, *Chem. Commun.*, 2015, **51**, 9797.
- 78 A. Berkefeld, W. E. Piers and M. Parvez, *J. Am. Chem. Soc.*, 2010, **132**, 10660.
- 79 M. Wen, F. Huang, G. Lu and Z.-X. Wang, *Inorg. Chem.*, 2013, **52**, 12098.
- 80 C. D. N. Gomes, E. Blondiaux, P. Thuéry and T. Cantat, *Chem.-Euro. J.*, 2014, **20**, 7098.
- 81 T. Wang and D. W. Stephan, *Chem.-Euro. J.*, 2014, **20**, 3036.
- 82 Y. Zhang, H. Zhang and K. Gao, *Org. Lett.*, 2021, **23**, 8282.
- 83 S. Das, R. C. Turnell-Ritson, P. J. Dyson and C. Corminboeuf, *Angew. Chem., Int. Ed.*, 2022, **61**, e202208987.
- 84 O. E. Palomero and R. A. Jones, *Dalton Trans.*, 2022, **51**, 6275.
- 85 L. Yang and H. Wang, *ChemSusChem*, 2014, **7**, 962.
- 86 S. Y.-F. Ho, C.-W. So, N. Saffon-Merceron and N. Mézailles, *Chem. Commun.*, 2015, **51**, 2107.
- 87 E. L. Kolychev, T. Bannenberg, M. Freytag, C. G. Daniliuc, P. G. Jones and M. Tamm, *Chem.-Euro. J.*, 2012, **18**, 16938.
- 88 E. Theuergarten, T. Bannenberg, M. D. Walter, D. Holschumacher, M. Freytag, C. G. Daniliuc, P. G. Jones and M. Tamm, *Dalton Trans.*, 2014, **43**, 1651.
- 89 J. Zeng, R. Qiu and J. Zhu, *Chem.-Asian. J.*, 2023, **18**, e20220123.
- 90 F. Lavigne, E. Maerten, G. Alcaraz, V. Branchadell, N. Saffon-Merceron and A. Baceiredo, *Angew. Chem., Int. Ed.*, 2012, **51**, 2489.
- 91 S. C. Sau, R. Bhattacharjee, P. K. Hota, P. K. Vardhanapu, G. Vijaykumar, R. Govindarajan, A. Datta and S. K. Mandal, *Chem. Sci.*, 2019, **10**, 1879.
- 92 S. C. Sau, Ra. Bhattacharjee, P. K. Vardhanapu, G. Vijaykumar, A. Datta and S. K. Mandal, *Angew. Chem., Int. Ed.*, 2016, **55**, 15147.
- 93 X. Chen, Y. Yang, H. Wang and Z. Mo, *J. Am. Chem. Soc.*, 2023, **145**, 7011.
- 94 N. D. Rio, M. Lopez-Reyes, A. Baceiredo, N. Saffon-Merceron, D. Lutters, T. Müller and T. Kato, *Angew. Chem., Int. Ed.*, 2017, **56**, 1365.
- 95 D. Wu, L. Kong, Y. Li, R. Ganguly and R. Kinjo, *Nat. Commun.*, 2015, **6**, 7340.
- 96 L. L. Liu, C. Chan, J. Zhu, C.-H. Cheng and Y. Zhao, *J. Org. Chem.*, 2015, **80**, 8790.
- 97 L. Kong, W. Lu, L. Yongxin, R. Ganguly and R. Kinjo, *Inorg. Chem.*, 2017, **56**, 5586.
- 98 M. P. Boone and D. W. Stephan, *Organometallics*, 2014, **33**, 387.
- 99 S. J. K. Forrest, J. Clifton, N. Fey, P. G. Pringle, H. A. Sparkes and D. F. Wass, *Angew. Chem., Int. Ed.*, 2015, **54**, 2223.
- 100 Y. Jiang, O. Blacque, T. Fox and H. Berke, *J. Am. Chem. Soc.*, 2013, **135**, 7751.
- 101 J. A. Buss, D. G. V. Velde and T. Agapie, *J. Am. Chem. Soc.*, 2018, **140**, 10121.
- 102 T. Zhao, X. Hu, Y. Wu and Z. Zhang, *Angew. Chem., Int. Ed.*, 2019, **58**, 722.
- 103 G. Menard and D. W. Stephan, *J. Am. Chem. Soc.*, 2010, **132**, 1796.
- 104 N. C. Smythe, D. A. Dixon, E. B. Garner, M. M. Rickard, M. Méndez, B. L. Scott, B. Zelenay and A. D. Sutton, *Inorg. Chem. Commun.*, 2015, **61**, 207.
- 105 C. Appelt, H. Westenberg, F. Bertini, A. W. Ehlers, J. C. Slootweg, K. Lammertsma and W. Uhl, *Angew. Chem., Int. Ed.*, 2011, **50**, 3925.
- 106 S. Roters, C. Appelt, H. Westenberg, A. Hepp, J. C. Slootweg, K. Lammertsma and W. Uhl, *Dalton Trans.*, 2012, **41**, 9033.
- 107 N. Aders, L. Keweloh, D. Pleschka, A. Hepp, M. Layh, F. Rogel and W. Uhl, *Organometallics*, 2019, **38**, 2839.
- 108 J. Boudreau, M. A. Courtemanche and F. G. Fontaine, *Chem. Commun.*, 2011, **47**, 11131.
- 109 H. S. Zijlstra, J. Pahl, J. Penafiel and S. Harder, *Dalton Trans.*, 2017, **46**, 3601.



- 110 P. Federmann, T. Bosse, S. Wolff, B. Cula, C. Herwig and C. Limberg, *Chem. Commun.*, 2022, **58**, 13451.
- 111 P. Federmann, R. Müller, F. Beckmann, C. Lau, B. Cula, M. Kaupp and C. Limberg, *Chem.–Euro. J.*, 2022, **28**, e2022004.
- 112 T. W. Yokley, H. Tupkar, N. D. Schley, N. J. DeYonker and T. P. Brewster, *Eur. J. Inorg. Chem.*, 2020, 2958.
- 113 M. Devillard, R. Declercq, E. Nicolas, A. W. Ehlers, J. Backs, N. Saffon-Merceron, G. Bouhadir, J. C. Slootweg, W. Uhl and D. Bourissou, *J. Am. Chem. Soc.*, 2016, **138**, 4917.
- 114 G. Menard and D. W. Stephan, *Dalton Trans.*, 2013, **42**, 5447.
- 115 (a) C. H. Lim, A. M. Holder, J. T. Hynes and C. B. Musgrave, *Inorg. Chem.*, 2013, **52**, 10062; (b) L. Roy, P. M. Zimmerman and A. Paul, *Chem.–Euro. J.*, 2011, **17**, 435; (c) P. M. Zimmerman, Z. Zhang and C. B. Musgrave, *Inorg. Chem.*, 2010, **49**, 8724.
- 116 (a) G. Menard, T. M. Gilbert, J. A. Hatnean, A. Kraft, I. Krossing and D. W. Stephan, *Organometallics*, 2013, **32**, 4416; (b) G. Menard and D. W. Stephan, *Angew. Chem., Int. Ed.*, 2011, **50**, 8396.
- 117 T. E. Stennett, J. Pahl, H. S. Zijlstra, F. W. Seidel and S. Harder, *Organometallics*, 2016, **35**, 207.
- 118 L. Wickemeyer, N. Aders, A. Mix, B. Neumann, H. G. Stammer, J. J. C. Trujillo, I. Fernandez and N. W. Mitze, *Chem. Sci.*, 2022, **13**, 8088.
- 119 W. Huang, T. Roisnel, V. Dorcet, C. Orione and E. Kirillov, *Organometallics*, 2020, **39**, 698.
- 120 M. D. Ramadhan and P. Surawatanawong, *Dalton Trans.*, 2021, **50**, 11307.
- 121 J. Chen, L. Falivene, L. Caporaso, L. Cavallo and E. Y.-X. Chen, *J. Am. Chem. Soc.*, 2016, **138**, 5321.
- 122 W. Uhl, M. Willeke, A. Hepp, D. Pleschka and M. Layh, *Z. Anorg. Allg. Chem.*, 2017, **643**, 387.
- 123 D. W. N. Wilson, J. Feld and J. M. Goicoechea, *Angew. Chem., Int. Ed.*, 2020, **59**, 20914.
- 124 D. A. Dickie, M. T. Barker, M. A. Land, K. E. Hughes, J. A. C. Clyburne and A. Kemp, *Inorg. Chem.*, 2015, **54**, 11121.
- 125 A. Schäfer, W. Saak, D. Haase and T. Müller, *Angew. Chem., Int. Ed.*, 2012, **51**, 2981.
- 126 M. Reißmann, A. Schäfer, S. Jung and T. Müller, *Organometallics*, 2013, **32**, 6736.
- 127 B. Waerder, M. Pieper, L. A. Körte, T. A. Kinder, A. Mix, B. Neumann, H. G. Stammer and N. W. Mitzel, *Angew. Chem., Int. Ed.*, 2015, **54**, 13416.
- 128 (a) S. Antoniotti, V. Dalla and E. Dunach, *Angew. Chem., Int. Ed.*, 2010, **49**, 7860; (b) B. Mathieu and L. Ghosez, *Tetrahedron*, 2002, **58**, 8219.
- 129 M. F. S. Valverde, E. Theuergarten, T. Bannenberg, M. Freytag, P. G. Jones and M. Tamm, *Dalton Trans.*, 2015, **44**, 9400.
- 130 N. von Wolff, G. Lefèvre, J.-C. Berthet, P. Thuéry and T. Cantat, *ACS Catal.*, 2016, **6**, 4526.
- 131 L. Wickemeyer, J. Schwabedissen, P. C. Trapp, B. Neumann, H.-G. Stammer and N. W. Mitzel, *Dalton Trans.*, 2023, **52**, 2611.
- 132 S. A. Weicker and D. W. Stephan, *Chem.–Euro. J.*, 2015, **21**, 13027.
- 133 (a) D. W. Stephan, *Science*, 2016, **354**, aaf7229; (b) D. W. Stephan, *Acc. Chem. Res.*, 2015, **48**, 306; (c) D. W. Stephan and G. Erker, *Angew. Chem., Int. Ed.*, 2015, **54**, 6400; (d) D. W. Stephan and G. Erker, *Angew. Chem., Int. Ed.*, 2010, **49**, 46.
- 134 (a) Q. Yang, L. Wang, Y. Li, L. Zhou and Z. Li, *J. Organomet. Chem.*, 2021, **954**, 122071; (b) T. A. Kinder, R. Pior, S. Blomeyer, B. Neumann, H.-G. Stammer and N. W. Mitzel, *Chem.–Euro. J.*, 2019, **25**, 5899.
- 135 P. Holtkamp, F. Friedrich, E. Stratmann, A. Mix, B. Neumann, H.-G. Stammer and N. W. Mitzel, *Angew. Chem., Int. Ed.*, 2019, **58**, 5114.
- 136 J. J. Cabrera-Trujillo and I. Fernandez, *J. Phys. Chem. A*, 2019, **123**, 10095.
- 137 P. Sarkar, S. Das and S. K. Pati, *J. Phys. Chem. C*, 2021, **125**, 22522.
- 138 A. Paparakis and M. Hulla, *ChemCatChem*, 2023, **15**, e202300510.
- 139 Z. W. Qu, H. Zhu and S. Grimme, *ChemCatChem*, 2020, **12**, 3656.
- 140 (a) I. Avigdori, K. Singh, A. Pogoreltsev, A. Kaushansky, N. Fridman and M. Gandelman, *Z. Anorg. Allg. Chem.*, 2023, **649**, e202200326; (b) I. Avigdori, A. Pogoreltsev, A. Kaushanski, N. Fridman and M. Gandelman, *Angew. Chem., Int. Ed.*, 2020, **59**, 23476; (c) J. Zhou, L. L. Liu, L. L. Cao and D. W. Stephan, *Chem. Commun.*, 2018, **54**, 4390.
- 141 L. J. Hounjet, C. B. Caputo and D. W. Stephan, *Angew. Chem., Int. Ed.*, 2012, **51**, 4714.
- 142 J. Zhu and K. An, *Chem.–Asian J.*, 2013, **8**, 3147.
- 143 A. Berkefeld, W. E. Piers, M. Parvez, L. Castro, L. Maron and O. Eisenstein, *Chem. Sci.*, 2013, **4**, 2152.
- 144 F. A. Le Blanc, W. E. Piers and M. Parvez, *Angew. Chem., Int. Ed.*, 2014, **53**, 789.
- 145 A. M. Chapman, M. F. Haddow and D. F. Wass, *J. Am. Chem. Soc.*, 2011, **133**, 18463.
- 146 O. J. Metters, S. J. K. Forrest, H. A. Sparkes, I. Manners and D. F. Wass, *J. Am. Chem. Soc.*, 2016, **138**, 1994.
- 147 X. Xu, G. Kehr, C. G. Daniliuc and G. Erker, *J. Am. Chem. Soc.*, 2013, **135**, 6465.
- 148 (a) C.-S. Wu and M.-D. Su, *Phys. Chem. Chem. Phys.*, 2023, **25**, 20618; (b) J. Z.-F. Zhang and M.-D. Su, *J. Phys. Chem. A*, 2022, **126**, 5534.
- 149 M. J. Sgro and D. W. Stephan, *Chem. Commun.*, 2013, **49**, 2610.
- 150 X. Xu, G. Kehr, C. G. Daniliuc and G. Erker, *J. Am. Chem. Soc.*, 2014, **136**, 12431.
- 151 J. M. V. Franco, G. Schnakenburg, T. Sasamori, A. E. Ferao and R. Streubel, *Chem.–Euro. J.*, 2015, **21**, 9650.
- 152 (a) S. Wesselbaum, T. vom Stein, J. Klankermayer and W. Leitner, *Angew. Chem., Int. Ed.*, 2012, **51**, 7499; (b) C. A. Huff and M. S. Sanford, *J. Am. Chem. Soc.*, 2011, **133**, 18122; (c) P. G. Jessop, T. Ikariya and R. Noyori, *Chem. Rev.*, 1995, **95**, 259.



- 153 M. J. Sgro and D. W. Stephan, *Angew. Chem., Int. Ed.*, 2012, **51**, 11343.
- 154 C. Cristóbal, Y. A. Hernández, J. López-Serrano, M. Paneque, A. Petronilho, M. L. Poveda, V. Salazar, F. Vattier, E. Álvarez, C. Maya and E. Carmona, *Chem.–Euro. J.*, 2013, **19**, 4003.
- 155 E. A. Romero, T. Zhao, R. Nakano, X. Hu, Y. Wu, R. Jazzar and G. Bertrand, *Nat. Catal.*, 2018, **1**, 743.
- 156 R. Dobrovetsky and D. W. Stephan, *Angew. Chem., Int. Ed.*, 2013, **52**, 2516.
- 157 R. Dobrovetsky and W. S. Douglas, *Isr. J. Chem.*, 2015, **54**, 206.
- 158 K. Chang, Y. Dong and X. Xu, *Chem. Commun.*, 2019, **55**, 12777.
- 159 K. K. Ghuman, T. E. Wood, L. B. Hoch, C. A. Mims, G. A. Ozin and C. V. Singh, *Phys. Chem. Chem. Phys.*, 2015, **17**, 14623.
- 160 K. K. Ghuman, L. B. Hoch, P. Szymanski, J. Y. Y. Loh, N. P. Kherani, M. A. El-Sayed, G. A. Ozin and C. V. Singh, *J. Am. Chem. Soc.*, 2016, **138**, 1206.
- 161 L. Wang, M. Ghossoub, H. Wang, Y. Shao, W. Sun, A. A. Tountas, T. E. Wood, H. Li, J. Y. Y. Loh, Y. Dong, M. Xia, Y. Li, S. Wang, J. Jia, C. Qiu, C. Qian, N. P. Kherani, L. He, X. Zhang and G. A. Ozin, *Joule*, 2018, **2**, 1369.
- 162 X. Liang, X. Wang, X. Zhang, S. Lin, M. Ji and M. Wang, *ACS Catal.*, 2023, **13**, 6214.
- 163 Y. Dong, K. K. Ghuman, R. Popescu, P. N. Duchesne, W. Zhou, J. Y. Y. Loh, F. M. Ali, J. Jia, D. Wang, X. Mu, C. Kübel, L. Wang, L. He, M. Ghossoub, Q. Wang, T. E. Wood, L. M. Reyes, P. Zhang, N. P. Kherani, C. V. Singh and G. A. Ozin, *Adv. Sci.*, 2018, **5**, 1700732.
- 164 J. Hao, Y. Zhang, L. Zhang, J. Shen, L. Meng and X. Wang, *Chem. Eng. J.*, 2023, **464**, 142536.
- 165 M. Ferrer, I. Alkorta, J. Elguero and J. M. Oliva-Enrich, *Sci. Rep.*, 2023, **13**, 2407.
- 166 T. G. Sentharamaikkannan, S. Krishnamurthy and S. Kaliaperumal, *New J. Chem.*, 2021, **45**, 9959.
- 167 X. Wang, L. Lu, B. Wang, Z. Xu, Z. Xin, S. Yan, Z. Geng and Z. Zou, *Adv. Funct. Mater.*, 2018, **28**, 1804191.
- 168 B. Chen and R. Neumann, *Eur. J. Inorg. Chem.*, 2018, 791.
- 169 C. Jia, X. Kan, X. Zhang, G. Lin, W. Liu, Z. Wang, S. Zhu, D. Ju and J. Liu, *Chem. Eng. J.*, 2022, **427**, 131554.
- 170 S. Zhang, Z. Xia, Y. Zou, F. Cao, Y. Liu, Y. Ma and Y. Qu, *J. Am. Chem. Soc.*, 2019, **141**, 11353.
- 171 D. Salusso, G. Grillo, M. Manzoli, M. Signorile, S. Zafeiratos, M. Barreau, A. Damin, V. Crocellà, G. Cravotto and S. Bordiga, *ACS Appl. Mater. Interfaces*, 2023, **15**, 15396.
- 172 (a) S. Zhang, Z. Tian, Y. Ma and Y. Qu, *ACS Catal.*, 2023, **13**, 4629; (b) Y. Xie, J. Chen, X. Wu, J. Wen, R. Zhao, Z. Li, G. Tian, Q. Zhang, P. Ning and J. Hao, *ACS Catal.*, 2022, **12**, 10587.
- 173 T. M. Rayder, F. Formalik, S. M. Vornholt, H. Frank, S. Lee, M. Alzayer, Z. Chen, D. Sengupta, T. Islamoglu, F. Paesani, K. W. Chapman, R. Q. Snurr and O. K. Farha, *J. Am. Chem. Soc.*, 2023, **145**, 11195.
- 174 Y. Jiang, X. Zhang and H. Fei, *Dalton Trans.*, 2020, **49**, 6548.
- 175 Y. Zhang, S. Chen, A. M. Al-Enizi, A. Nafady, Z. Tang and S. Ma, *Angew. Chem., Int. Ed.*, 2023, **62**, e202213399.
- 176 R. Declercq, G. Bouhadir, D. Bourissou, M.-A. Légaré, M.-A. Courtemanche, K. S. Nahi, N. Bouchard, F.-G. Fontaine and L. Maron, *ACS Catal.*, 2015, **5**, 2513.

